AD-A061 430 MISSION RESEARCH CORP SANTA BARBARA CALIF F/G 18/3
REQUIREMENTS FOR IMPROVED INFRARED PREDICTION CAPABILITY. HAES --ETC(U)
APR 78 D H ARCHER DNA001-77-C-0227
UNCLASSIFIED MRC-R-383 DNA-4585F NL

1 OF 2
AD
A061 430

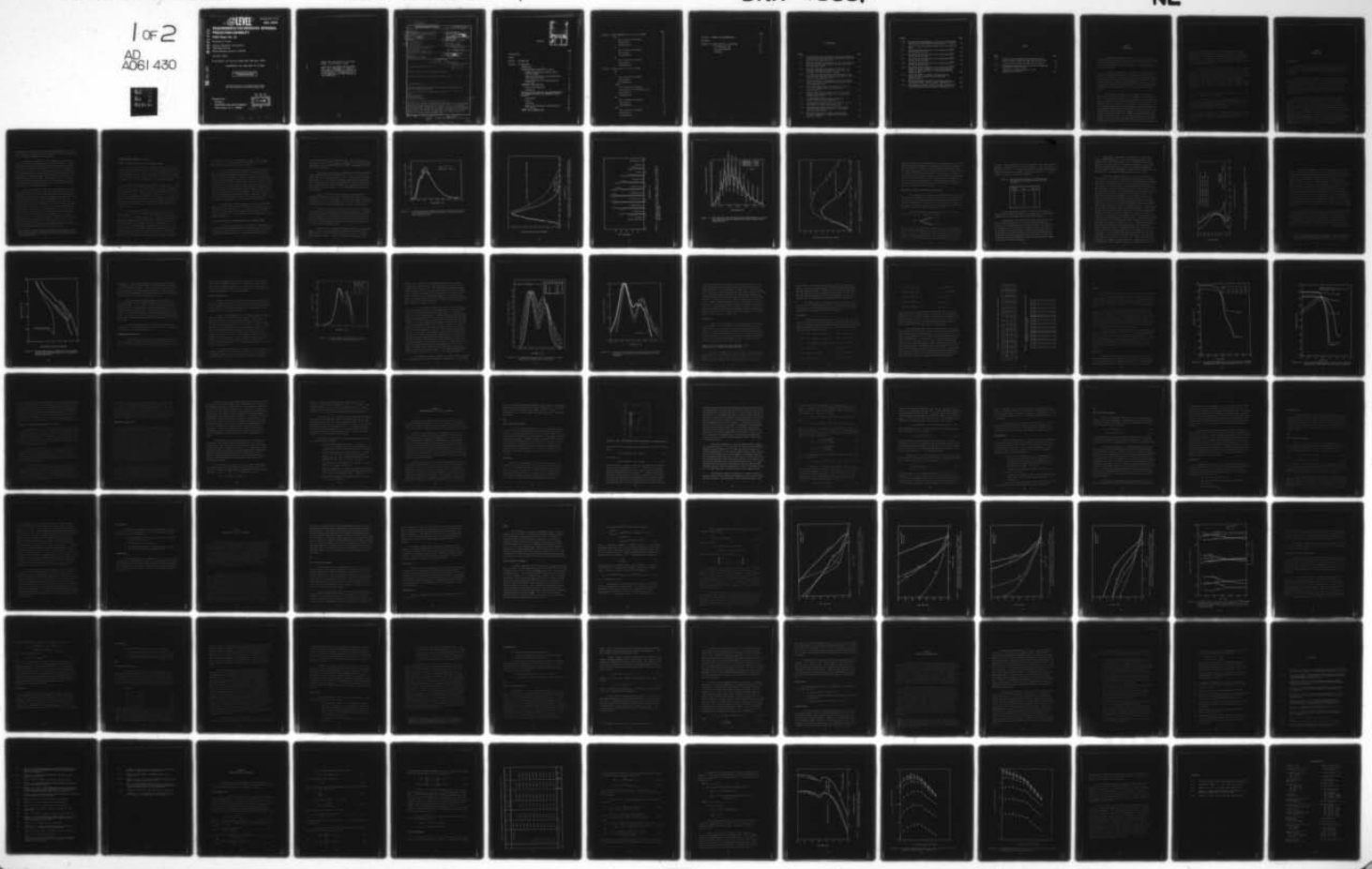

(12) LEVEL II

AD-E300 367

DNA 4585F

REQUIREMENTS FOR IMPROVED INFRARED PREDICTION CAPABILITY

HAES Report No. 78

Douglas H. Archer

Mission Research Corporation
735 State Street
Santa Barbara, California 93102

30 April 1978

Final Report for Period 4 May 1977—30 April 1978

CONTRACT No. DNA 001-77-C-0227

THIS WORK SPONSORED BY THE DEFENSE NUCLEAR AGENCY
UNDER RDT&E RMSS CODE B322077464 S99QAXHI00246 H2590D.

Prepared for
Director
DEFENSE NUCLEAR AGENCY
Washington, D. C. 20305

Destroy this report when it is no longer needed. Do not return to sender.

PLEASE NOTIFY THE DEFENSE NUCLEAR AGENCY, ATTN: TISI, WASHINGTON, D.C. 20305, IF YOUR ADDRESS IS INCORRECT, IF YOU WISH TO BE DELETED FROM THE DISTRIBUTION LIST, OR IF THE ADDRESSEE IS NO LONGER EMPLOYED BY YOUR ORGANIZATION.

(18) DNA, SBIE (19) 4585F; AD-E300 367

UNCLASSIFIED

SECURITY CLASSIFICATION OF THIS PAGE (When Data Entered)

REPORT DOCUMENTATION PAGE

READ INSTRUCTIONS BEFORE COMPLETING FORM

1. REPORT NUMBER: DNA 4585F

2. GOVT ACCESSION NO.

3. RECIPIENT'S CATALOG NUMBER

(6) 4. TITLE (and Subtitle): REQUIREMENTS FOR IMPROVED INFRARED PREDICTION CAPABILITY, HAES Report No. 78 N umber 78.

(9) 5. TYPE OF REPORT & PERIOD COVERED: Final Report, [redacted]d 4 May [redacted]77—30 Apr[redacted]78,

(14) 6. PERFORMING ORG. REPORT NUMBER: MRC-R-383

7. AUTHOR(s): (10) Douglas H. Archer

(15) 8. CONTRACT OR GRANT NUMBER(s): DNA 001-77-C-0227

9. PERFORMING ORGANIZATION NAME AND ADDRESS: Mission Research Corporation, 735 State Street, Santa Barbara, California 93101

10. PROGRAM ELEMENT, PROJECT, TASK AREA & WORK UNIT NUMBERS: (16) NWED Subtask S99QAXH002-46

11. CONTROLLING OFFICE NAME AND ADDRESS: Director, Defense Nuclear Agency, Washington, D.C. 20305

12. REPORT DATE: 30 Apr[redacted]78

13. NUMBER OF PAGES: 100

14. MONITORING AGENCY NAME & ADDRESS (if different from Controlling Office): (12) 98p.

15. SECURITY CLASS (of this report): UNCLASSIFIED

15a. DECLASSIFICATION/DOWNGRADING SCHEDULE

16. DISTRIBUTION STATEMENT (of this Report): (17) I0002

Approved for public release; distribution unlimited.

17. DISTRIBUTION STATEMENT (of the abstract entered in Block 20, if different from Report)

18. SUPPLEMENTARY NOTES

This work sponsored by the Defense Nuclear Agency under RDT&E RMSS Code B322077464 S99QAXH100246 H2590D.

19. KEY WORDS (Continue on reverse side if necessary and identify by block number)

Aurora
Infrared Prediction
Infrared Radiation
Uncertainties (Infrared)

micrometers

20. ABSTRACT (Continue on reverse side if necessary and identify by block number)

This report describes work performed to determine the major uncertainties involved in the prediction of infrared radiation in the 2- to 5-μm region following atmospheric nuclear bursts. Emphasis is placed on wavelength bands near 2.8 and 4.3 μm. Specifically included for consideration are the molecular species NO, CO_2, CO, OH, HO_2, H_2O, H_2O_2, HNO_2, HNO_3, $N^{14}N^{15}$, NO+, and N_2O. A priority listing is provided of recommended research items necessary for improvement of our prediction capability.

DD FORM 1 JAN 73 1473 EDITION OF 1 NOV 65 IS OBSOLETE

UNCLASSIFIED

SECURITY CLASSIFICATION OF THIS PAGE (When Data Entered)

78 10 05 050

406 548

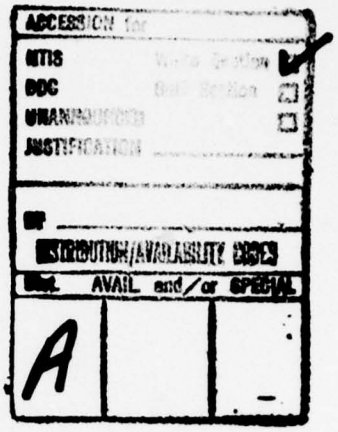

CONTENTS

ILLUSTRATIONS

TABLES

SECTION 1
INTRODUCTION

Nuclear-induced infrared radiation in the 2- to 5-μm region has important systems (and potential systems) implications. This is especially true for wavelength bands near 2.8 and 4.3 μm. Accurate modeling of the emissions is necessary for a good assessment of the systems degradation in a nuclear environment.

In the work reported here, we attempt to pinpoint the major uncertainties currently associated with a determination of the molecular emissions, particularly those near 2.8 and 4.3 μm, and recommend a research effort designed to improve the prediction accuracy. Emphasis is placed on the chemical/optical phenomena associated with the excitation and emission. Uncertainties related to nuclear phenomenology, that in some instances may overshadow those considered here, lie outside the scope of the present effort.

The procedure adopted was to first identify the atmospheric molecules that are known to radiate in the wavelength regions of interest. Next, we attempted to evaluate the relative importance of each specie in a nuclear environment by considering various pieces of field, laboratory, and theoretical data. In particular, use was made of prior MHD/chemistry code runs for high-altitude bursts, D-region chemistry benchmark calculations, and comparisons with Fishbowl and auroral data. Certain species have been eliminated from consideration on the grounds that their formation rates, compared with those for other species radiating at nearly the same wavelength, are relatively small. For those species retained, we have established a list of the major uncertainties and have assigned, for each molecule, relative priorities relating to the need for research to reduce them.

Finally, we have attempted to provide an overall priority listing of research requirements, taking into consideration the relative importance of each specie and the systems needs, or anticipated needs, as we currently understand them. The ordering of priorities is necessarily somewhat subjective since systems requirements, in terms of wavelength bands, sensitivity, etc., are subject to change.

Section 2 is devoted to a consideration of NO which has long been believed to be the major source of 2.8- and 5.4-μm emission in a nuclear environment. The chemiluminescent and atom-interchange excitation mechanisms are reviewed in the light of existing field data —both auroral and nuclear. Deficiencies in the models used to describe the data are identified. The sensitivity of NO chemiluminescence to the unknown branching ratios for production of $N(^4S)$ and $N(^2D)$ atoms, under nuclear-disturbed conditions, is quantified and recommendations are made for specific laboratory measurements.

Section 3 considers other emitters in the 2.6- to 2.9-μm region with special emphasis on CO_2, OH, and HO_2.

Section 4 deals with the wavelength band from about 4.1 to 4.6 μm. Included for consideration are the molecules CO_2, CO, $N^{14}N^{15}$, NO^+, and NO_2, some of which may produce nuclear-enhanced emission in the blue- or red-spike regions of the main CO_2 absorption band.

Finally, Section 5 gives a summary of our findings and presents a priority listing of recommended field, laboratory, and theoretical research programs required to upgrade our modeling capability for the 2- to 5-μm region.

SECTION 2
NO RADIATION

INTRODUCTION

This section discusses various aspects of the problem of verifying the mechanisms involved in the generation of IR radiation from NO, the uncertainties associated with its prediction, and recommendations for specific measurements.

Because NO radiation in a nuclear environment has important systems implications, a major goal of DNA programs, including ICECAP, EXCEDE, COCHISE, and LABCEDE, has been the verification of weapon-effects models used to describe this radiation. Uncertainty in the mechanisms, and in certain parameters involved in the mechanisms, has persisted, although the above programs have served to advance our knowledge of them and to decrease the uncertainties accordingly.

Until the advent of the auroral program ICECAP, the dominant excitation mechanism for NO fundamental and overtone radiation outside hot fireballs was believed to be chemiluminescence, especially through the $N(^2D) + O_2$ reaction. However, analysis of ICECAP has shown that, although the limited amount of auroral data near 2.7 μm can approximately be accounted for on this basis, the data near 5.4 μm cannot. On the other hand, it appears that earthshine scatter from NO, coupled with excitation of $NO(v=1)$ by the atom-interchange reaction $O' + NO \rightarrow O + NO'$, can, in the main, account for the results. But no confirmation of this is available since the concentrations of NO and O were not directly measured. Confirmation of the atom-interchange mechanism has potentially important systems applications in a nuclear

environment where the temperature may be sufficiently elevated, over large spatial regions, to produce excitation of NO(v=2) with emission intensities at 2.7 μm approaching thermal equilibrium values.*

Validation or improvement of the chemiluminescent model for NO emission has also been an important goal in the past few years. A significant forward step in this effort has been the recent COCHISE measurements at AFGL on the vibrational distribution of NO following its formation by the $N(^2D) + O_2$ reaction. This work establishes the spectral distribution of the emitted NO radiation and provides a good estimate (probably to within a few percent) of the absolute photon efficiency for the reaction in both the fundamental and overtone bands. These results can be used to update previous calculations of auroral intensities, and comparisons with ICECAP data, and to learn more about the relative roles of chemiluminescence and atom interchange in exciting NO emission.

In this section we first look at the COCHISE results on the relative production rates of NO(v) by the $N(^2D) + O_2$ reaction and report an independent verification of the spectral distribution of radiated energy and the photon efficiency for both the fundamental and overtone bands. The significance of these results on prior chemiluminescent calculations, particularly those relating to auroral conditions, is discussed. This has bearing on the next topic which concentrates on the 5.4-μm spectral region. Here we compare some theoretical results on the spectral distribution of (1,0) band emission from NO, at various temperatures, with CVF (circular variable filter) data from ICECAP. The implications of these comparisons, relative to the atom-interchange and the chemiluminescent excitation mechanisms, is discussed. Finally, we report on the results of some calculations performed to determine the sensitivity of NO chemistry and chemiluminescence to the branching ratios for the formation of $N(^4S)$ and $N(^2D)$. Recommendations are then made for laboratory and field experiments to upgrade our prediction capabilities for IR emission from NO.

---

* This statement is based on work performed under this contract, but not otherwise reported here, in which the results of former MHD calculations for a high-yield, high-altitude burst were modified to include the atom-interchange mechanism.

CHEMILUMINESCENCE FROM $N(^2D) + O_2 \rightarrow NO + O$

Photons Per Reaction and Sensitivity to Quenching Models

In Appendix A we present an independent calculation of the photon efficiency in the fundamental and first overtone bands of NO, excited by the reaction $N(^2D) + O_2 \rightarrow NO + O$, using the recently measured data by AFGL on the relative production rates for NO(v). Included are the effects of quenching using two different models. The principal results are presented in Table A-1 and Figures A-1 to A-3. The conclusions can be summarized as follows.

In the zero quenching limit, the number of photons, $\eta_{fund.}$, emitted per reaction by NO in the fundamental band is 3.9; the number, $\eta_{overtone}$, in the first overtone band is 0.28. Above about 80-km altitude, quenching by atomic oxygen dominates and produces relative minima at 100 km in the altitude profiles for $\eta_{fund.}$ and $\eta_{overtone}$. The values for η then increase with increasing altitude and approach their zero quenching limits above about 140 km. Below 80 km, the photon efficiencies decrease nearly exponentially with decreasing altitude, because of quenching by molecular oxygen, so that at 20 km they are about three orders of magnitude smaller than their unquenched values.

The quenching models adopted assume that the quenching rate constants satisfy either (i) quenching proportional to the vibrational quantum number, v, i.e., $k_{v,v-1} = vk_{1,0}$, or (ii) quenching independent of v, i.e., $k_{v,v-1} = k_{1,0}$. Model 1 provides for considerably more quenching of the higher vibrational states than does Model 2. Nevertheless, for the fundamental band, the two models produce nearly identical values for η. For the first overtone band, Model 2 quenching gives values for η about 70 percent larger than does Model 1 quenching at 20-km altitude, but the differences decrease with increasing altitude. Thus, we conclude that although the magnitude of the quenching rate constant $k_{1,0}$ is important, knowledge of the relative rates among the different vibrational states is

not particularly crucial to a determination of $\eta_{fund.}$ and $\eta_{overtone}$. Thus, use of $k_{1,0}$ as a quenching rate constant for all states NO(v) probably gives sufficient accuracy for most purposes.

As far as emission from the individual vibration-rotation (V-R) bands of the first overtone band system of NO is concerned, our results show that with Model 1 quenching, the peak emission occurs in the (5,3) band (2.81 μm) at all altitudes. For Model 2 quenching, however, there is a shift in the band for which the peak emission occurs. Above about 120 km, it occurs in the (5,3) band. From 115 to at least 80 km, it occurs in the (6,4) band (2.86 μm), and at and below 50 km, the peak is in the (7,5) band (2.90 μm). Thus, at lower altitudes, Model 2 quenching should produce a shift in the overtone spectrum toward longer wavelengths, perhaps by about 0.1 μm, relative to that at the higher altitudes. However, as we will see below, the chemiluminescent overtone spectrum is sufficiently broad (≈ 0.3 μm full width at half maximum) so that if such a shift occurs, and is ignored, no significant calculational error in the intensity should result.

Based upon the foregoing calculations, employing two quenching models, we conclude that detailed measurement of the variation with v of the quenching rate coefficient $k_{v,v-1}$, relative to $k_{1,0}$, is probably not critical for a determination of the nuclear-induced interference with systems operating near 2.7 μm and, therefore, that such measurements do not warrant top priority.

Spectral Distribution of Emitted Radiation (Zero Quenching Limit)

In earlier reports (Reference 2-1, Appendix A, and Reference 2-2) we calculated the NO chemiluminescent spectra from the $N(^2D) + O_2$ reaction based on the assumption that the first 18 vibrational states of NO are populated with equal probability. Using the same procedures, we have

recalculated the spectra using the COCHISE data. These calculations were done only for the case of zero quenching, although use of the results, shown in Appendix A, in our computer routine will permit a determination of the spectra for any altitude.

The procedure used is to first calculate the fraction of the total number of photons emitted by the band system ($\Delta v = 1$ or $\Delta v = 2$) whose wavelength falls in a resolution element, $\Delta\lambda$, at λ. This produces a bar graph which would, if $\Delta\lambda$ were chosen small enough, exhibit all the rotational lines of the band system. Next, we simulate what a circular variable filter (CVF) spectrometer, of effective bandwidth, $\Delta\lambda_{CVF}$, would see as it scans in wavelength over the bar spectrum. It is these synthetic CVF spectra that are shown here.

Figure 2-1 shows the calculated spectral distribution of NO fundamental band photons per reaction in a band of width $\Delta\lambda_{CVF} = 0.12$ μm. A resolution $\Delta\lambda = 0.02$ μm was adopted. The results are shown for rotational temperatures of 250 and 450 °K, although for $\lambda > 5.6$ μm the two results are indistinguishable. Note that the peak emission occurs at about 5.45 μm.

In Figure 2-2 the 250 °K curve of Figure 2-1 has been converted to a "per micron" basis by dividing by 0.12 and the resulting curve is compared with the corresponding result obtained on the basis of our old "equal population" assumption. We see that the new and old spectra are quite similar at short wavelengths up to the peak, but thereafter the old spectrum falls off more slowly with wavelength because of the assumed greater production rate of the higher vibrational states.

Figures 2-3 to 2-5 present the results for the first overtone band. Figure 2-3 shows the wavelength positions and relative strengths of the peaks of the R, Q, and P branches of the bands in the $\Delta v = 2$ sequence at a temperature of 300 °K. Figure 2-4 shows spectra calculated for two

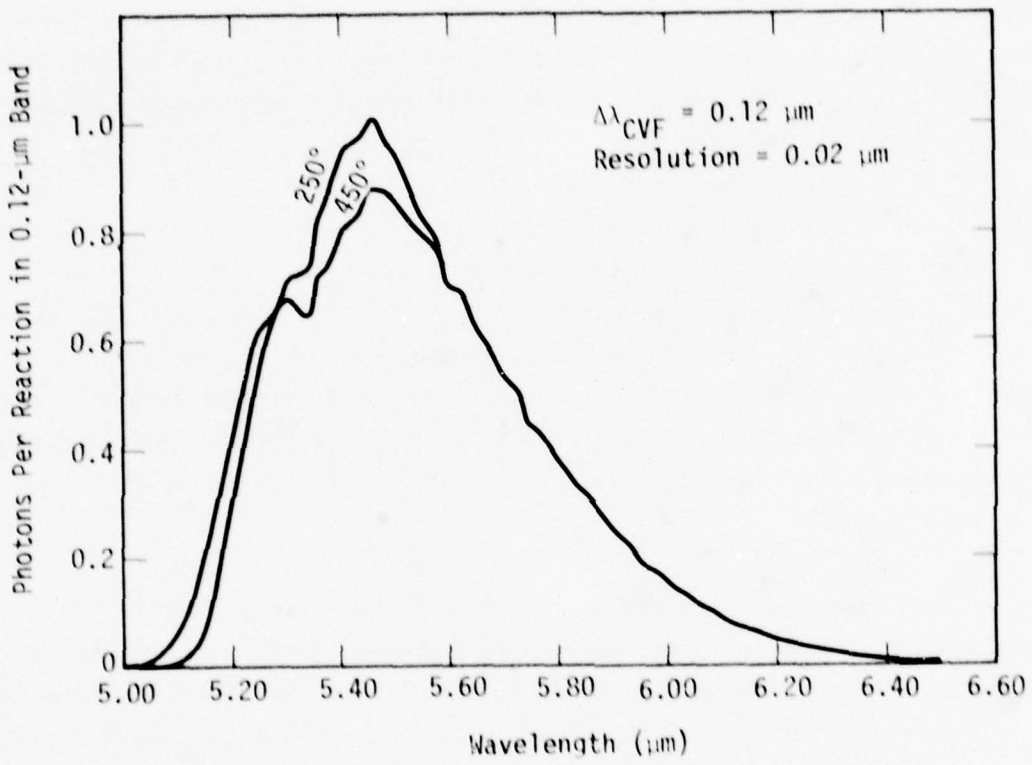

Figure 2-1. Calculated spectrum (fundamental) of NO chemiluminescence using the AFGL laboratory data for the $N(^2D) + O_2 \rightarrow NO + O$ reaction (zero quenching limit).

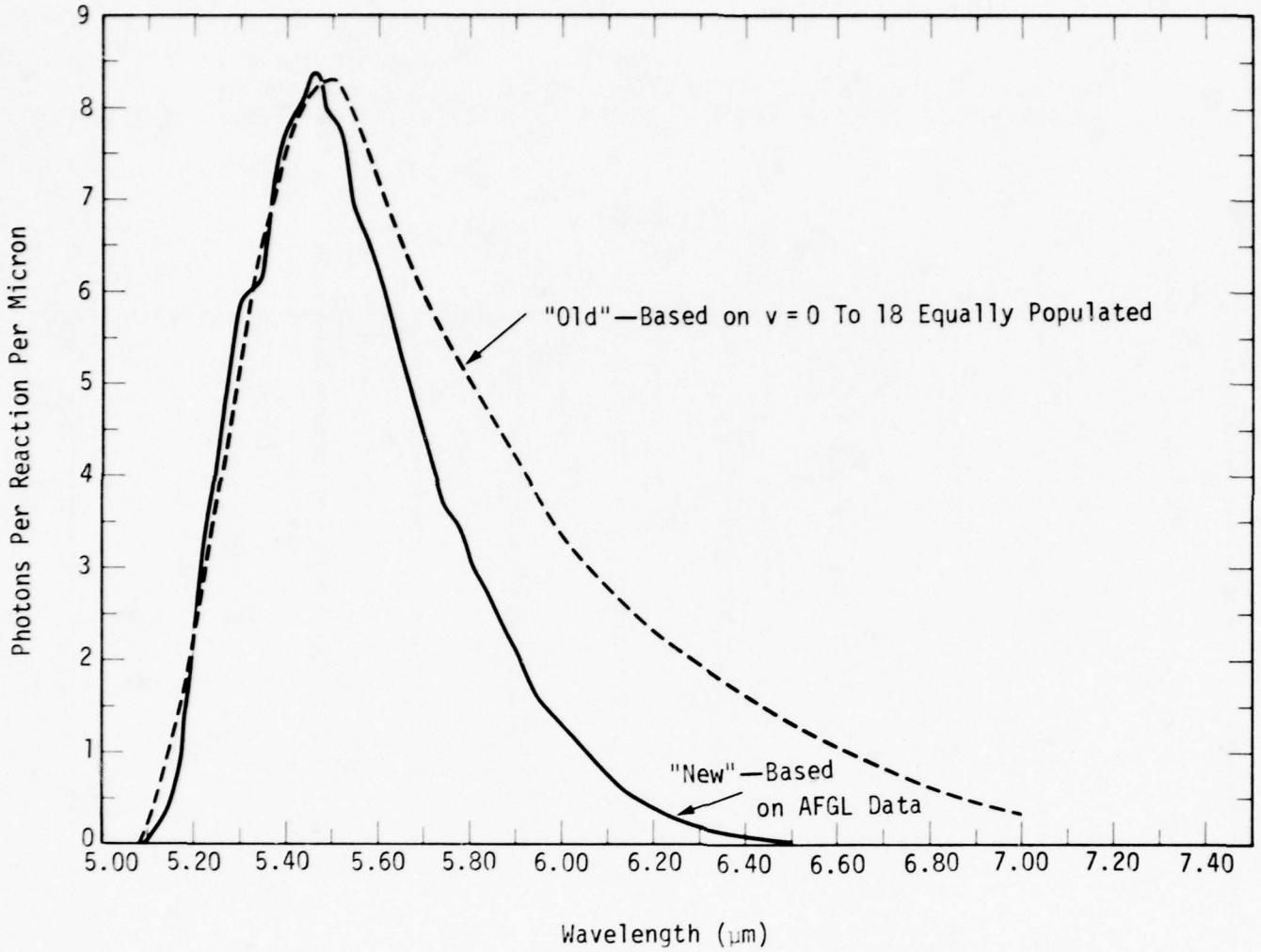

Figure 2-2. Comparison between old and new spectra for NO fundamental emission from the reaction $N(^2D) + O_2 \rightarrow NO + O$ at 250 K°(zero quenching limit).

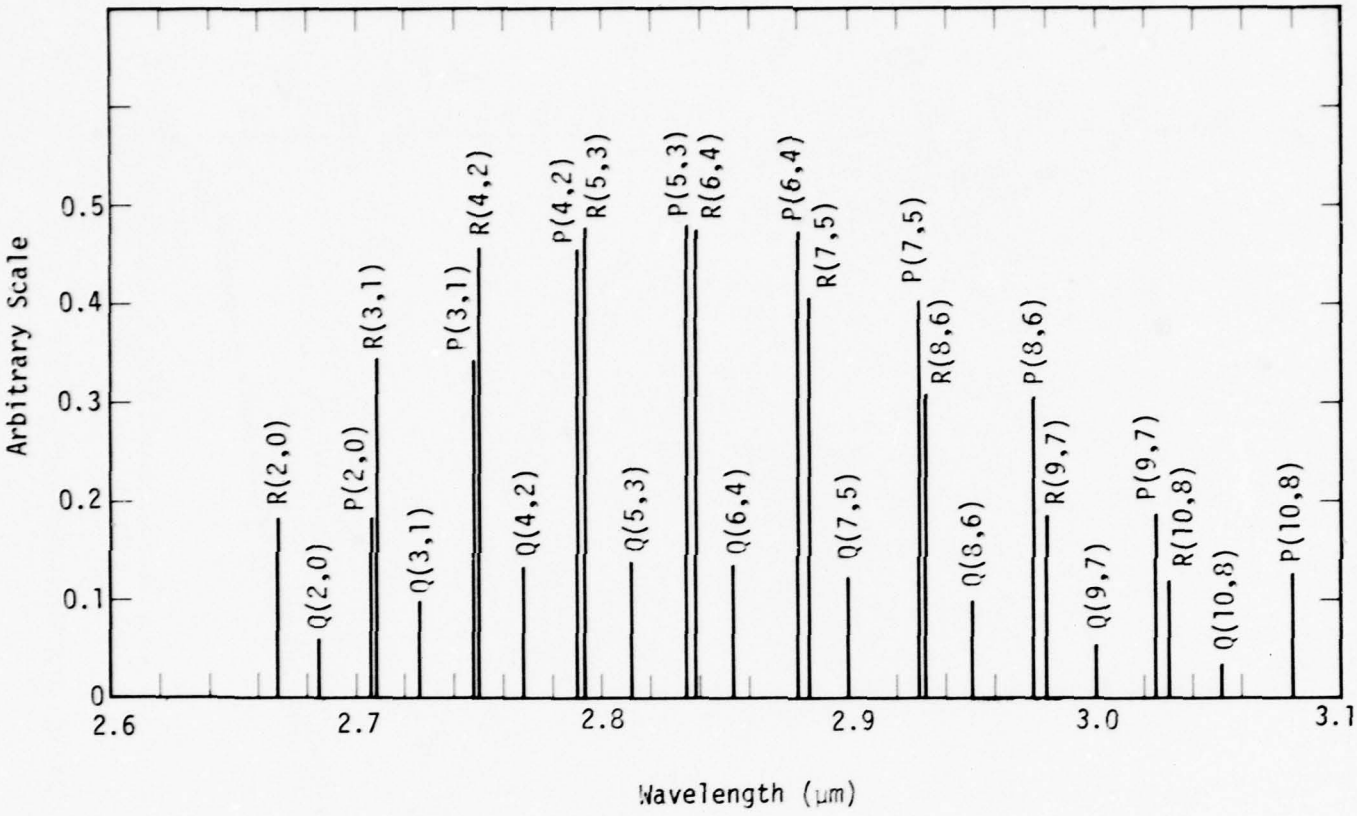

Figure 2-3. Positions and relative strengths of peaks of R, Q, P branches of NO overtone transitions in steady state from $N(^2D) + O_2 \rightarrow NO + O$ reaction at 300°K.

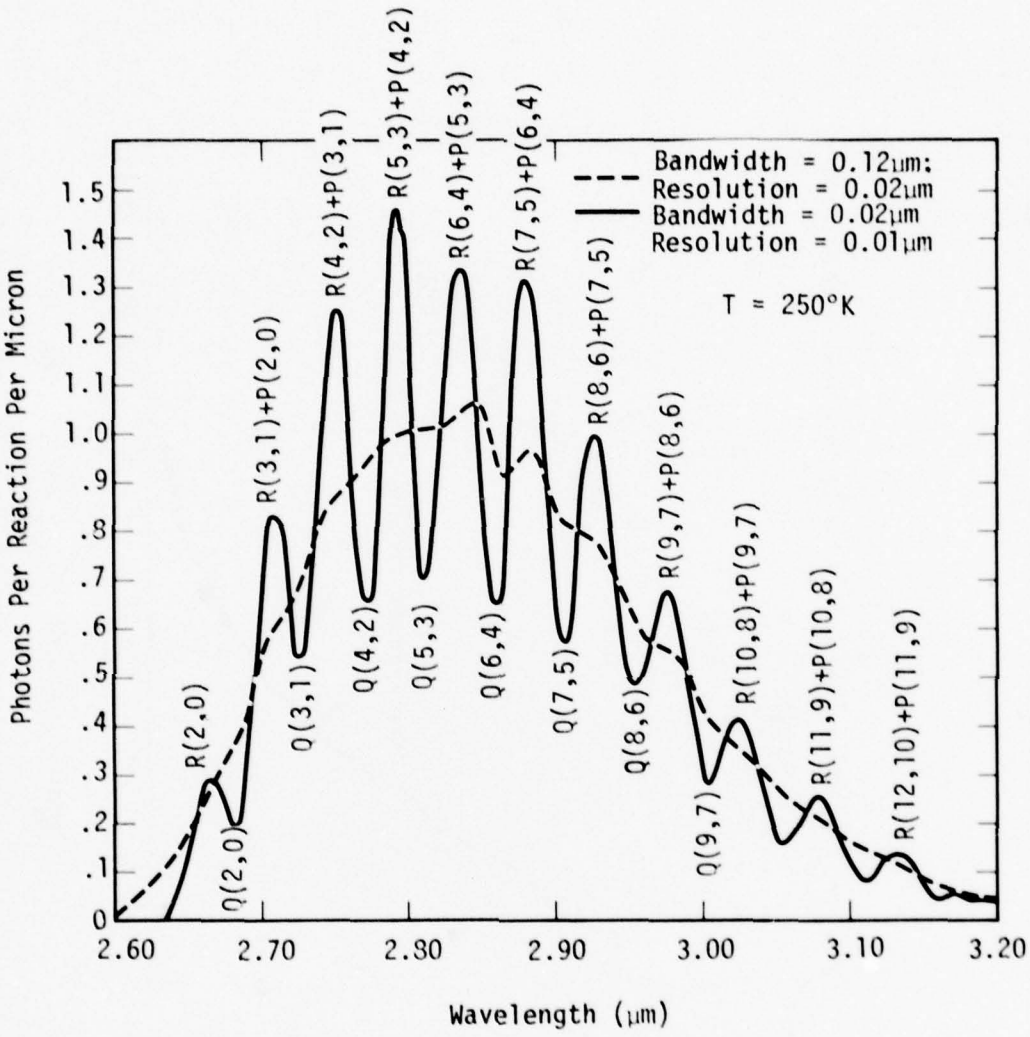

Figure 2-4. Calculated spectrum (overtone) of NO chemiluminescence using the AFGL laboratory data for the $N(^2D) + O_2 \rightarrow NO + O$ reaction (zero quenching limit).

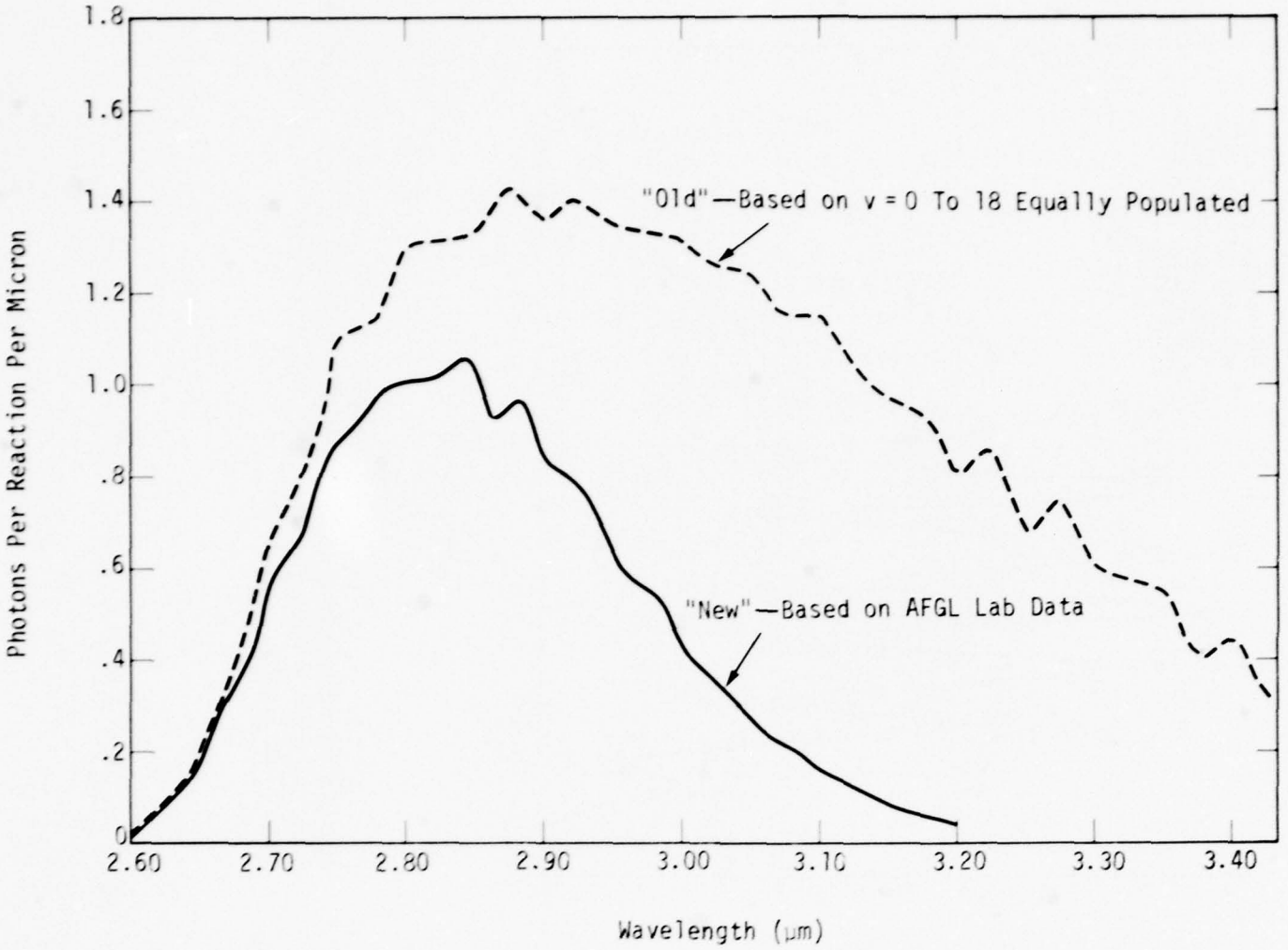

Figure 2-5. Comparison between old and new spectra for NO overtone emission from the reaction $N(^2D) + O_2 \rightarrow NO + O$ at 250°K (zero quenching limit).

different combinations of CVF bandwidth, $\Delta\lambda_{CVF}$, and resolution, $\Delta\lambda$, at 250°K. For the spectrum corresponding to the higher resolution, the individual peaks are identified according to the main bands that contribute to them. The relative strengths of some of the peaks shown may not be accurate because of insufficiently small values chosen for $\Delta\lambda$ and $\Delta\lambda_{CVF}$. In Figure 2-5 we compare the low resolution spectrum of Figure 2-4 with the corresponding spectrum calculated on the basis of the "equal population" assumption. As can be seen, the new spectrum peaks at a somewhat shorter wavelength, and exhibits considerably fewer photons at and beyond the rather broad peak near 2.84 μm, than does the old spectrum.

Implications to Prior Calculations and Conclusions

The foregoing results, pertaining to photon efficiency and spectral emission for the fundamental and overtone bands of NO, can be compared with those used in prior calculations, particularly those using the ARCTIC code. We have reviewed some of our earlier work, in light of the above changes, to see what conclusions, if any, based on previous comparisons with auroral ICECAP data, and nuclear Fishbowl data, need revision.

The former calculations assumed that the $N(^2D) + O_2$ reaction forms $O(^3P)$ and $O(^1D)$ according to the scheme

$$N(^2D) + O_2 \xrightarrow{4 \times 10^{-12}} NO + O(^3P)$$

$$N(^2D) + O_2 \xrightarrow{2 \times 10^{-12}} NO + O(^1D)$$

which, with the "equal population" assumption, results in 5.7 fundamental photons and 0.82 overtone photons per overall reaction with a rate constant of 6×10^{-12} cm^3 sec^{-1}. These numbers are to be compared with the new ones, based on COCHISE measurements, of 3.9 and 0.28, respectively. Thus, our assumed η values for the fundamental and overtone were high by factors

of about 1.5 and 2.9 compared with the new unquenched values. When collisional quenching is included, Table 2-1, based on Figure A-1, shows, for selected altitudes, the factors, F, by which our previously calculated chemiluminescent volume emission rates are too large. The overtone values for F are based on Model 2 quenching as described in Appendix A.

Table 2-1. Factors by which previously calculated auroral NO chemiluminescent volume emission rates are too large.

Altitude (km)	$F_{fund.}$	$F_{overtone}$
90	2.2	4.1
100	4.0	6.4
110	2.6	4.3
120	1.9	3.4
130	1.6	3.2
∞	1.5	2.9

We have applied these factors to correct our previous calculations and to reconsider the conclusions regarding the role of NO chemiluminescence in the interpretation of nuclear and auroral data.

Nuclear Data. The IR data from two high-altitude bursts have been reviewed with the object of verifying the NO chemiluminescent mechanism for the fundamental and first overtone bands. After applying the foregoing results on spectral band shapes and photon efficiencies, and allowing for instrument response functions and transmission losses, we find that in one case the data are consistent with the NO mechanism. In the other case they are decidedly not. We conclude, therefore, that the nuclear data do not unambiguously support the conventionally assumed role for NO in a nuclear environment.

Auroral Data. With respect to auroral data, the conclusions formerly reached (Reference 2-3) were: (1) NO chemiluminescence cannot account for the bulk of the data near 5.4 μm, either with respect to the magnitude of the emission or to its spectral distribution; (2) the calculated NO chemiluminescence near 2.7 μm is in reasonable agreement with the only available rocket measurement of zenith intensity (rocket A10.205-2, 24 March 1973). Our comments on these conclusions are as follows.

First, with respect to Conclusion 2, the new spectral distribution (Figure 2-5) is in better agreement with the CVF data on this flight (see Figure 3-12, Reference 2-2) than is the old "equal population" spectrum. However, our new calculated zenith intensity (modified from Reference 2-2) falls short by a factor of about 3 in accounting for the rocket data above 95-km altitude. As to the fluorescence efficiency (on an energy basis) in the 2.8-μm band, Figure 2-6 is a graphical summary of our theoretical results for several auroral events compared with the available field data. The theoretical curves have incorporated the recent COCHISE results on the $N(^2D) + O_2$ reaction and also quenching as shown in Figure A-1. The rocket data shown in Figure 2-6 was obtained by integrating over the CVF spectral features (near 2.8 μm) at 75- and 100-km altitudes and using the measured 3914-Å zenith intensity to infer the energy deposition rate. One other piece of rocket data (not shown), from a side looking radiometer on ICECAP rocket A18.205-1, has been used by Kofsky (Reference 2-4) to infer a fluorescence efficiency as high as 3.5 percent. However, because of the necessity of subtracting a large earth-limb contribution to the observed radiance in this case, the associated uncertainty is probably large. The range of efficiencies inferred from the 2.8-μm aircraft data, shown in Figure 2-6, was obtained from analyses presented in References 2-4 to 2-6. Although the theoretical efficiencies are functions of altitude and depend on the input auroral particle spectrum as well as the bombardment time (since it takes time to achieve steady state conditions after turn-on of the aurora), it is clear from Figure 2-6 that the theoretical values are generally less than about 0.3 percent. The field data, on the other hand, support values that are larger than this by factors of at least 2 to 3. Clearly, more field data and analyses are needed to confirm whether NO overtone emission can fully account for the auroral intensity and spectral distribution near 2.7 μm.

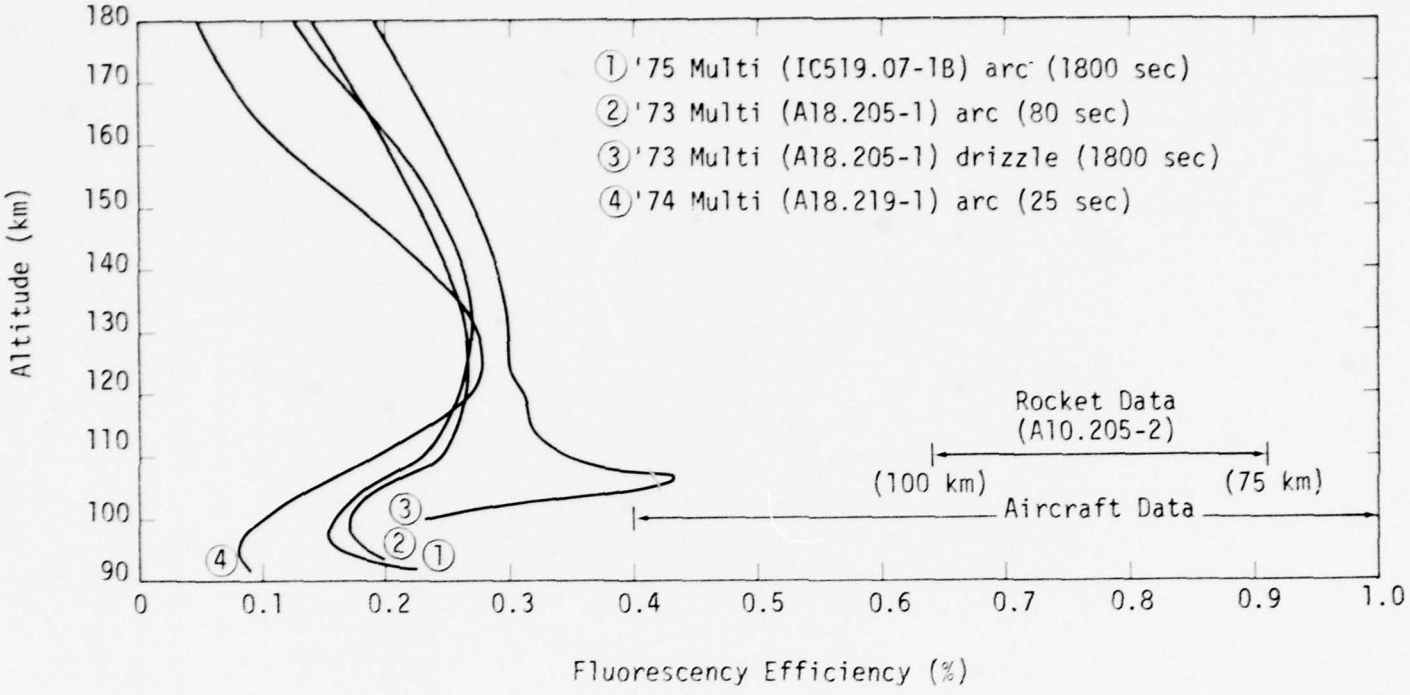

Figure 2-6. Calculated (ARCTIC code) fluorescence efficiency at 2.7 μm using COCHISE data for the reaction $N(^2D) + O_2 \rightarrow NO + O$.

Next, for the fundamental band, we looked primarily at CVF data from the '75 Multi event (rocket IC519.07-1B). This is because the instrument used for that event extended in wavelength to 5.6 μm and so permitted observations to wavelengths beyond the peak of the feature near 5.4 μm which the earlier instrumented flights did not. The feature actually exhibits a double peak (see, for example, Figure 2-13, Reference 2-3) the main one at about 5.2 μm and the other at about 5.4 μm. Figure 2-7 shows the zenith spectral intensity for these peaks measured on rocket ascent. As far as we can infer, the arc was above the rocket until the rocket penetrated it at about 125-km altitude. Details of this event, and our earlier calculations, are presented in Reference 2-3. The calculated peak spectral radiance near 5.4 μm, as inferred from Figure 2-2 and our ARCTIC code calculations, is shown by the dashed curve in Figure 2-7. It is seen that the calculated values at low altitudes are within a factor of 2 of those measured for the 5.4-μm peak and, above 130 km, actually exceed the measured values.

The comparison shown in Figure 2-7 is at variance with our former Conclusion 1 above and, if taken seriously, presents a dilemma in terms of spectral interpretation as discussed in the next subsection. However, it should perhaps be noted here, that although our calculations were based on the measured input particle flux to the aurora, our calculated zenith intensity profile for 3914 Å exceeds the measured one by factors between about 2 and 4 (see Figure 2-10, Reference 2-3).* If the theoretical curve

* This discrepancy between intensities measured at 3914 Å by photometers and those inferred from particle measurements is consistent with comparisons made for other auroral events, but its source is not known.

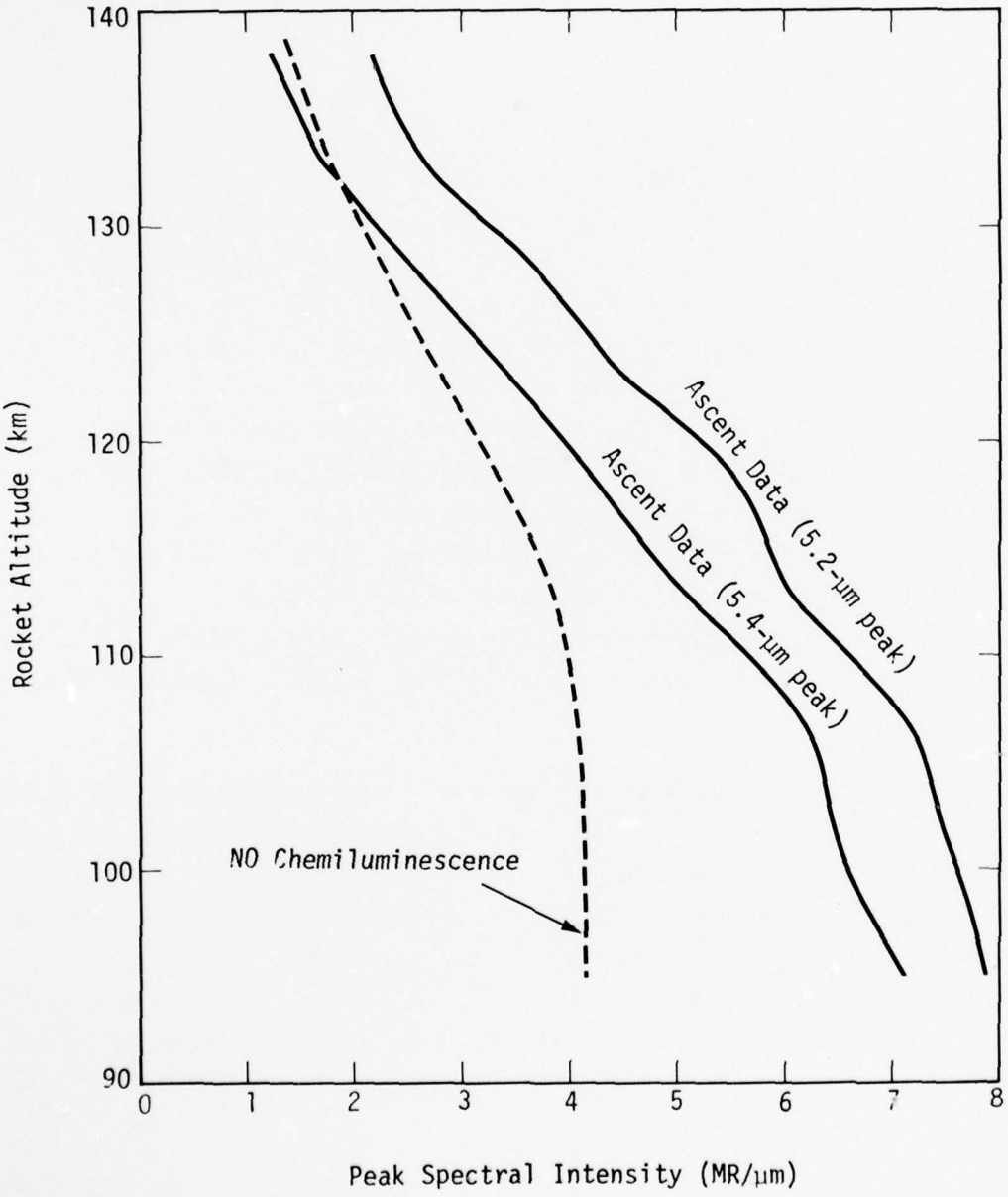

Figure 2-7. Observed peak spectral radiance for 5.3-μm features compared with calculated values for the auroral arc (rocket IC519.07-1B).

in Figure 2-7 is thus reduced accordingly, the measured peak intensity at 5.4 μm would exceed the calculated peak by factors of about 4 at 100 km, 3.5 at 115 km, and 3 at 130 km. In any case, for later reference, we note that the calculations show that at higher altitudes, a larger fraction of the emission is attributable to NO chemiluminescence than it is at the lower altitudes, at least for this particular auroral event.

The explanation for the double peak of the 5.3-μm feature, as given in Reference 2-3, and further elaborated in the next subsection, is that they are the R and P branches of the (1,0) band of NO excited, presumably, by the atom-interchange reaction and earthshine scatter. If, on the other hand, chemiluminescence, *with a single peak near 5.4 μm* (see Figure 2-2) is the major contributor, it would leave unexplained the source of the 5.2-μm peak and also the near symmetry in the 5.3-μm zenith intensity that has been consistently observed on ICECAP flights during rocket ascent and descent.

In the next subsection we look in detail at some measured CVF spectra near 5.3 μm and further discuss the implications of a substantial contribution to it from NO chemiluminescence.

FUNDAMENTAL BAND RADIATION

As indicated earlier in this section, the auroral data near 5.4 μm can, in principle, be accounted for largely on the basis of NO(v=1) excitation by a combination of the atom-interchange reaction and earthshine scatter

provided the NO concentration is suitably enhanced over its low-latitude values (see, for example, Reference 2-3). Excitation of NO(v=2), with implications to systems operating near 2.7 μm, can similarly be expected in regions of the atmosphere heated by nuclear explosions. Validation of the atom-interchange mechanism is therefore important.

Spectral Considerations

We have seen in the last subsection that our auroral calculations for the '75 Multi event (IC 519.07-1B) give an NO chemiluminescent contribution to the fundamental band that is at least a substantial fraction of the measured intensity. The question of whether this is compatible with the *available CVF spectra will now be examined.*

Figure 2-8 (from Reference A-4 or 2-7) shows co-added CVF spectra taken on ascent at selected altitudes and presented such that the 5.2-μm peaks are all normalized to unit relative intensity. As pointed out in References A-4 and 2-7, three features to note about the spectra are that with increasing altitude there is: (1) a shift of the 5.2-μm peak to shorter wavelengths, (2) a decrease in the 5.4-μm peak relative to the 5.2-μm peak, and (3) a narrowing of the entire structure. In References A-4 and 2-7, features 2 and 3 were presented as evidence that NO chemiluminescence is operating to modify the 5.4-μm peak at altitudes below 140 km. Thus, presumably, the spectrum in Figure 2-8 corresponding to an altitude of 137 km represents (1,0) band radiation from NO. At lower altitudes, NO chemiluminescence, with a peak near 5.4 μm, would serve to enhance the 5.4-μm peak relative to that at 5.2 μm.

The foregoing explanation of the features is at least qualitatively appealing. However, there are difficulties with it. First, we find, from an independent study of the CVF data, that the variation with altitude of the ratio between the two peaks is about the same on rocket ascent and

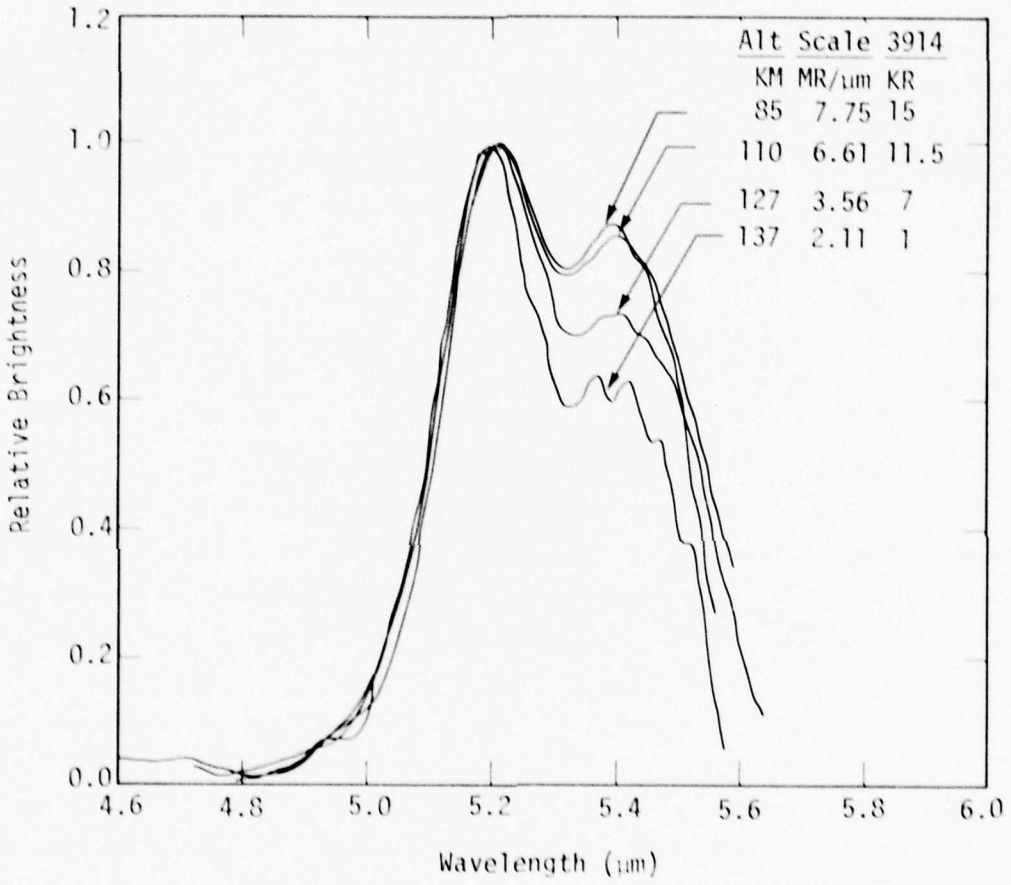

Figure 2-8. Co-added normalized CVF data on ascent from rocket IC519.07-1B (from Reference 2-7).

descent. But, according to the on-board 3914-Å photometer, the rocket descended in a region where the auroral intensity was at least ten times less than that on rocket ascent. Thus, the relative contribution from NO chemiluminescence to the 5.4-μm peak should be much less on descent than on ascent. Second, as was pointed out in the previous subsection, our calculations indicate that for the particular auroral arc in question, chemiluminescence should become relatively more important at the higher altitudes than at the lower altitudes (see Figure 2-7). This is just the reverse of what is needed to account for feature 2.

There is an alternative explanation, however, that fits features 1 and 2 (although not feature 3) that we now present. It is based on the fact that for increasing altitude above 100 km, there is a monotonic increase in the kinetic temperature, T. Assuming Boltzmann equilibrium among the rotational states, this reflects itself in a change with altitude in the ratio of R- to P-branch peaks of the (1,0) band of NO. We have calculated synthetic CVF spectra (assumed CVF bandwidth of 0.12 μm) for the (1,0) band at selected temperatures between 250 and 750 °K. The results, with the R branches normalized to the same value, are shown in Figure 2-9. The top curve (250 °K) corresponds to an altitude of about 110 km; the bottom one (750 °K) to an altitude of about 160 km. Notice the shift of the R-branch peak near 5.2 μm to shorter wavelengths with increasing T (altitude) and also the decrease in magnitude of the P-branch peak near 5.4 μm relative to that of the R branch. The latter effect is due partly to the increasing wavelength separation of the peaks with increasing T, coupled with the fact that the transition probability for each rotational line varies as ν^4. Figure 2-10 compares 550 °K and 750 °K spectra from Figure 2-9 with the co-added CVF feature at 137 km from Figure 2-8. The latter should correspond to emission from altitudes above 137 km, i.e., to temperatures $\gtrsim$600 °K.

The resemblance between the measured CVF features and the calculated (1,0) band spectra of NO, shown in Figures 2-8 through 2-10, is sufficiently

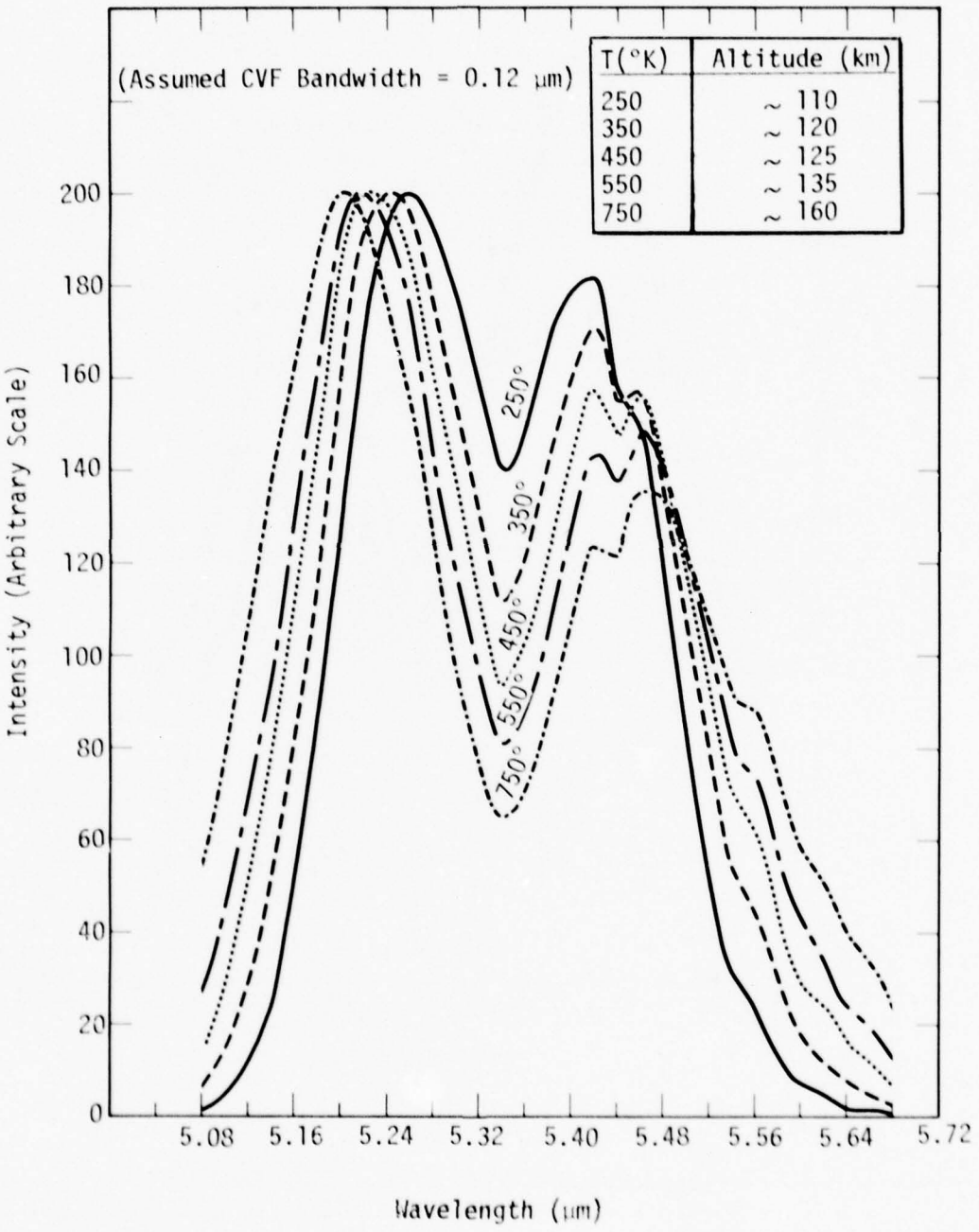

Figure 2-9. Calculated CVF spectrum of NO (1,0) band for several temperatures (R-branch peaks normalized).

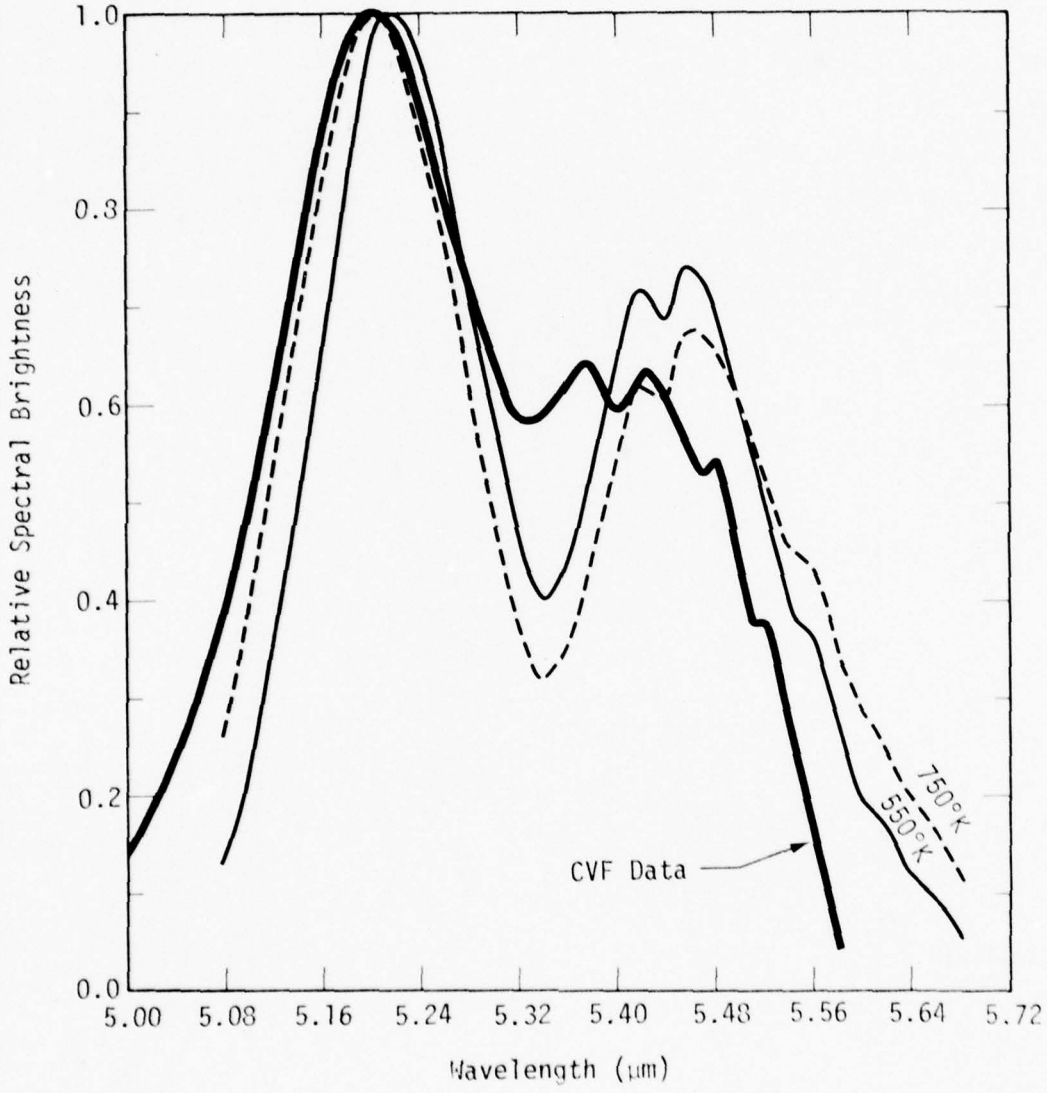

Figure 2-10. Calculated CVF spectrum of NO (1,0) band at two different temperatures normalized to co-added CVF data at 137-km altitude.

striking to add considerable weight to the idea that the emission is completely dominated by the NO(1,0) band excited by atom interchange plus earthshine scatter. On the other hand, if Figure 2-8 is a true representation of the facts, then the explanation just given doesn't entirely fit either. First, unless the rotational states are far from Boltzmann populated, the band should broaden with increasing altitude (as in Figure 2-9) rather than narrowing. Second, the 5.4-μm peaks should be somewhat larger, relative to the 5.2-μm peaks, than those shown in Figure 2-8, especially at the lower temperatures. Third, if we attribute a substantial fraction of the emission near 5.4 μm to chemiluminescence ($\gtrsim$30 percent at 130 km) as the previous subsection suggests we should, then the measured 5.4-μm peak should be even greater, relative to the 5.2-μm peak, than shown in Figure 2-9. The data in Figure 2-8 shows that this is not the case.

Conclusions

There are clearly problems involved in attempting to explain the CVF spectra near 5.3 μm based either on a model that assumes only (1,0) band radiation from NO (the atom-interchange and earthshine scatter mechanisms) or else one that includes a contribution from NO chemiluminescence. Because of the potential importance of NO emission to systems, we recommend that this situation be clarified at an early date. Hopefully, the planned field-widened interferometer experiment will provide auroral data with sufficient resolution to resolve these questions.

SENSITIVITY OF NO CHEMISTRY AND CHEMILUMINESCENCE TO THE BRANCHING RATIOS FOR FORMATION OF $N(^4S)$ AND $N(^2D)$

The rate of formation of NO and, consequently, the NO chemiluminescent intensity, are dependent on the relative concentrations of $N(^4S)$ and $N(^2D)$ atoms. This is because $N(^4S)$ and $N(^2D)$ react with O_2 to form NO at quite different rates except at temperatures above about

1500 to 2000 °K. The relative concentrations of the two nitrogen species depends, in turn, on the branching ratios for their formation by several different chemical reactions. Included are dissociative recombination in N_2^+ and NO^+, the ion-atom interchange reaction between N_2^+, and O to form NO^+, and prompt formation by electron bombardment. Only for NO^+ recombination has laboratory data on the branching ratio been obtained.

The purpose of the work reported here is to determine the sensitivity of the NO chemiluminescence, and NO concentration, to variations (uncertainties) in the various branching ratios and, if necessary, to make recommendations for appropriate laboratory measurements.

Calculations

In order to determine the degree of sensitivity of the NO chemistry to uncertainties in the various branching ratios, we numerically solved the set of 7 nonlinear differential equations that describe the time dependent species concentrations ($N(^4S)$, $N(^2D)$, NO, N_2^+, O_2^+, NO^+, O^+) for the following simplified set of chemical reactions:

$$N_2^+ + e \xrightarrow{k_1} f_1 N(^4S) + (2-f_1) N(^2D) \quad ; \; k_1 = 8.8 \times 10^{-7} \; T^{-0.2}$$

$$NO^+ + e \xrightarrow{k_2} f_2 N(^4S) + (1-f_2) N(^2D) + O \quad ; \; k_2 = 3.5 \times 10^{-6} \; T^{-0.37}$$

$$N_2^+ + O \xrightarrow{k_3} f_3 N(^4S) + (1-f_3) N(^2D) + NO^+ \quad ; \; k_3 = 1.6^{-9} \; T^{-0.44}$$

$$O_2^+ + e \xrightarrow{k_4} O + O \quad ; \; k_4 = 1.2^{-5} \; T^{-0.7}$$

$$O^+ + N_2 \xrightarrow{k_5} NO^+ + N(^4S) \quad ; \; k_5 = 1.2^{-10} \; T^{-0.8}$$

$$O^+ + O_2 \xrightarrow{k_6} O_2^+ + O \quad ; \; k_6 = 3.5^{-10} \; T^{-0.5}$$

$$N_2^+ + O_2 \xrightarrow{k_7} N_2 + O_2^+ \qquad ; k_7 = 8.6^{-10}\ T^{-0.5}$$

$$N(^4S) + O_2 \xrightarrow{k_8} NO + O \qquad ; k_8 = 2.4^{-11}\ e^{-3980/T}$$

$$N(^4S) + NO \xrightarrow{k_9} N_2 + O \qquad ; k_9 = 2.2^{-11}$$

$$N(^2D) + O_2 \xrightarrow{k_{10}} NO + O \qquad ; k_{10} = 6.0^{-12}$$

$$N(^2D) + NO \xrightarrow{k_{11}} N_2 + O \qquad ; k_{11} = 5.9^{-11}$$

Here, f_1, f_2, and f_3 are the branching ratios for $N(^4S)$ and $N(^2D)$ production by the first three reactions. In addition, we assume that one nitrogen atom per ion pair is created by the prompt X rays (Reference 2-8) with a fraction f_4 in the ^4S state and $(1-f_4)$ in the ^2D state. An ambient ionosphere was also provided along with a background ionization source consistent with the assumed ambient electron density.

Some calculations were done for an altitude of 90 km, but most were done for 110 km. The initial values adopted for species concentrations and the ambient electron production rate, q_e, are shown in Table 2-2. In Table 2-2 the parameter f is the initial fractional ionization created by prompt energy deposition. Values used for f, the fractional ionization were 3.5×10^{-3} at 90 km and 2×10^{-2} at 110 km. For the 110-km altitude, calculations were made using branching ratio combinations shown in Table 2-3. These were performed for temperatures of 266, 500, and 1500 °K, a total of 72 separate calculations, each run for times out to 100 sec. For the 90-km altitude, runs were made using six different branching ratio combinations and a temperature of 184 °K. Only the 110-km results are described here since they span the range of variations observed at both altitudes.

Table 2-2. Initial values used for the chemistry calculations.

Altitude (km)	$[N_2^+]$ (cm^{-3})	$[O_2^+]$ (cm^{-3})	[NO] (cm^{-3})	$[O^+]$ (cm^{-3})	$[N^4S]$ (cm^{-3})	$[N^2D]$ (cm^{-3})	[NO] (cm^{-3})	$[N_2]$ (cm^{-3})	$[O_2]$ (cm^{-3})	[O] (cm^{-3})	N_e (cm^{-3})	(q_e) ($cm^3\ sec^{-1}$)
90	$5.5^{13}f$	$1.1^{13}f$	10.0	$5.2^{12}f$	$7.1^{13}ff_4$	$7.1^{13}f(1-f_4)$	2.9^7	5.6^{13}	1.4^{13}	1.7^{11}	$7.1^{13}f$	1.28^3
110	$1.7^{12}f$	$2.0^{11}f$	10.0	$1.2^{11}f$	$2.2^{12}ff_4$	$2.2^{12}f(1-f_4)$	9.5^7	1.6^{12}	2.5^{11}	3.2^{11}	$2.0^{12}f$	1.76^4

Table 2-3. Combination of branching ratios for which calculations performed at 110-km altitude.

f_1	f_2	f_3	f_4	f_1	f_2	f_3	f_4	f_1	f_2	f_3	f_4
1.5	.25	.5	.5	1.5	.75	.75	.75	.25	.25	.25	1.0
1.0	.25	.5	.5	.25	.25	.25	.25	.25	.25	1.0	.25
.5	.25	.5	.5	.5	.25	.5	.25	1.0	.25	.5	0.0
1.0	.25	.25	.5	.5	0.0	.5	.25	1.0	.25	.25	.25
1.0	.25	.75	.5	.5	.25	.25	.25	.5	.5	.5	.25
1.0	.25	.5	.25	.25	.25	.5	.25	.5	.25	.5	1.0
1.0	.25	.5	.75	0.0	.25	.25	.25	.25	.25	.5	1.0
1.5	.25	.75	.75	.25	.25	.5	.5	.25	.25	.25	.5

Results

For the limited cases run, the results can be summarized as follows:

1. At a temperature of 1500 °K, the rate at which NO is formed by reaction between O_2 and either $N(^4S)$ or $N(^2D)$ is sufficiently similar that the species concentrations and NO chemiluminescence are quite insensitive to changes in any of the branching ratios. The same remarks apply for T > 1500 °K.

2. For T = 266 and 500 °K, the results are most sensitive to changes in f_1 and f_4. For example, a factor of 2 increase in f_1 (for fixed values of the other f^S) can lead to a decrease in [NO] by a factor of 600 at 266 °K and an increase in the chemiluminescence by a factor of 35 at 500 °K. Similarly, a change in f_4 by a factor of 2 can lead to corresponding changes in [NO] and in the chemiluminescence by factors of 5000 and 100, respectively. Variation of f_2 or f_3 results in considerably less change in either [NO] or the chemiluminescence.

3. Of the cases run, the largest variation in the chemiluminescence, for f_2 set equal to the laboratory value (0.25), occurred for simultaneous variation of f_1, f_3, and f_4. The results are shown in Figures 2-11 and 2-12. From Figure 2-11 we see that at 100 sec there is more than a 3 order of magnitude difference in the chemiluminescence between the two cases. Correspondingly, from Figure 2-12 we see that the difference in [NO] is nearly 2 orders of magnitude and, in $[N(^4S)]$, it is over 5 orders of magnitude.

Conclusions

The foregoing results show that, at least under conditions where the fractional ionization is reasonably high ($\gtrsim 10^{-15}[O]$), but the temperature is below about 1500 °K, relatively small errors in the assumed branching ratios for production of $N(^4S)$ and $N(^2D)$ by N_2^+ recombination,

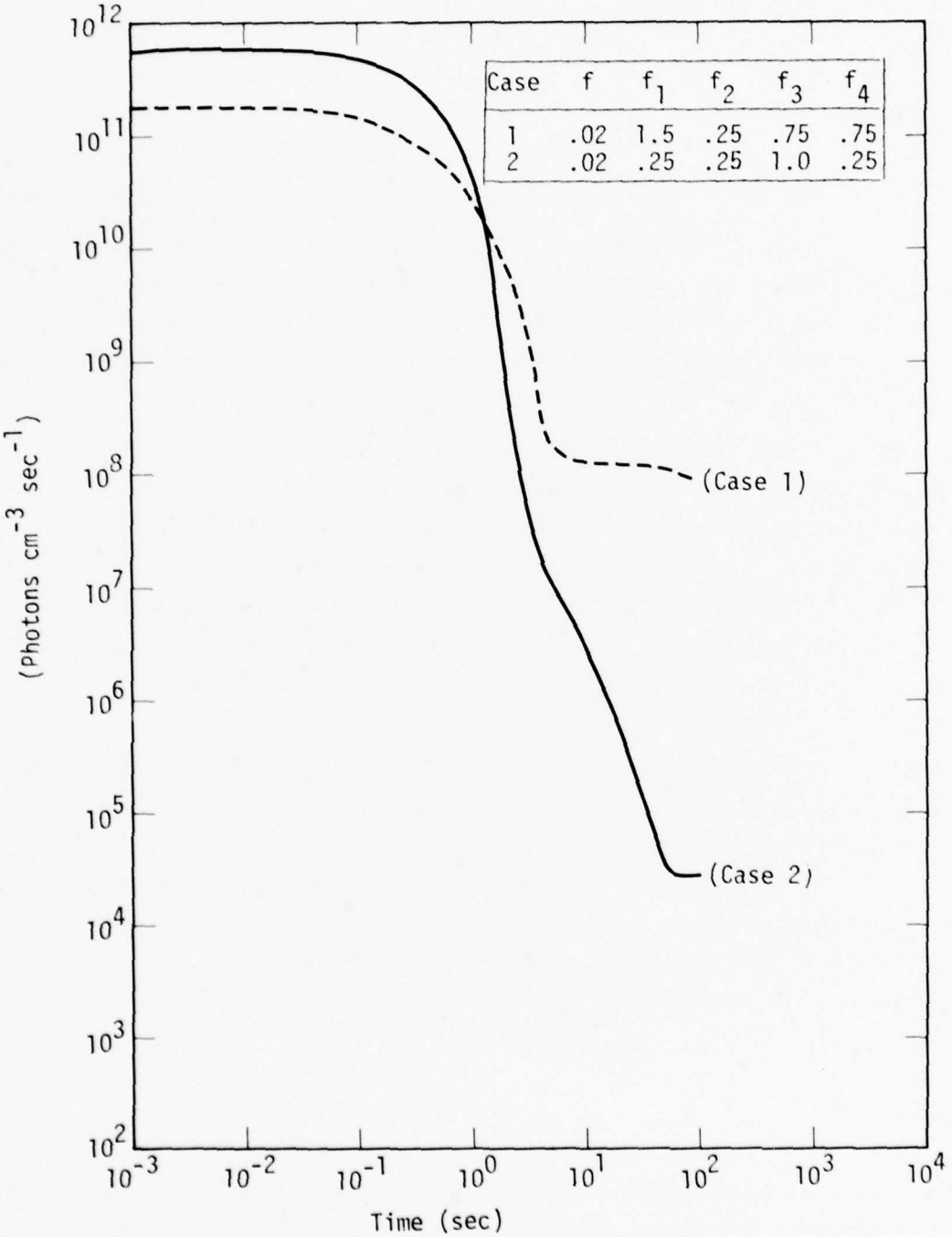

Figure 2-11. NO chemiluminescence (5.4 μm) at 110 km for two different combinations of $N(^4S)/N(^2D)$ branching ratios (T = 500°K).

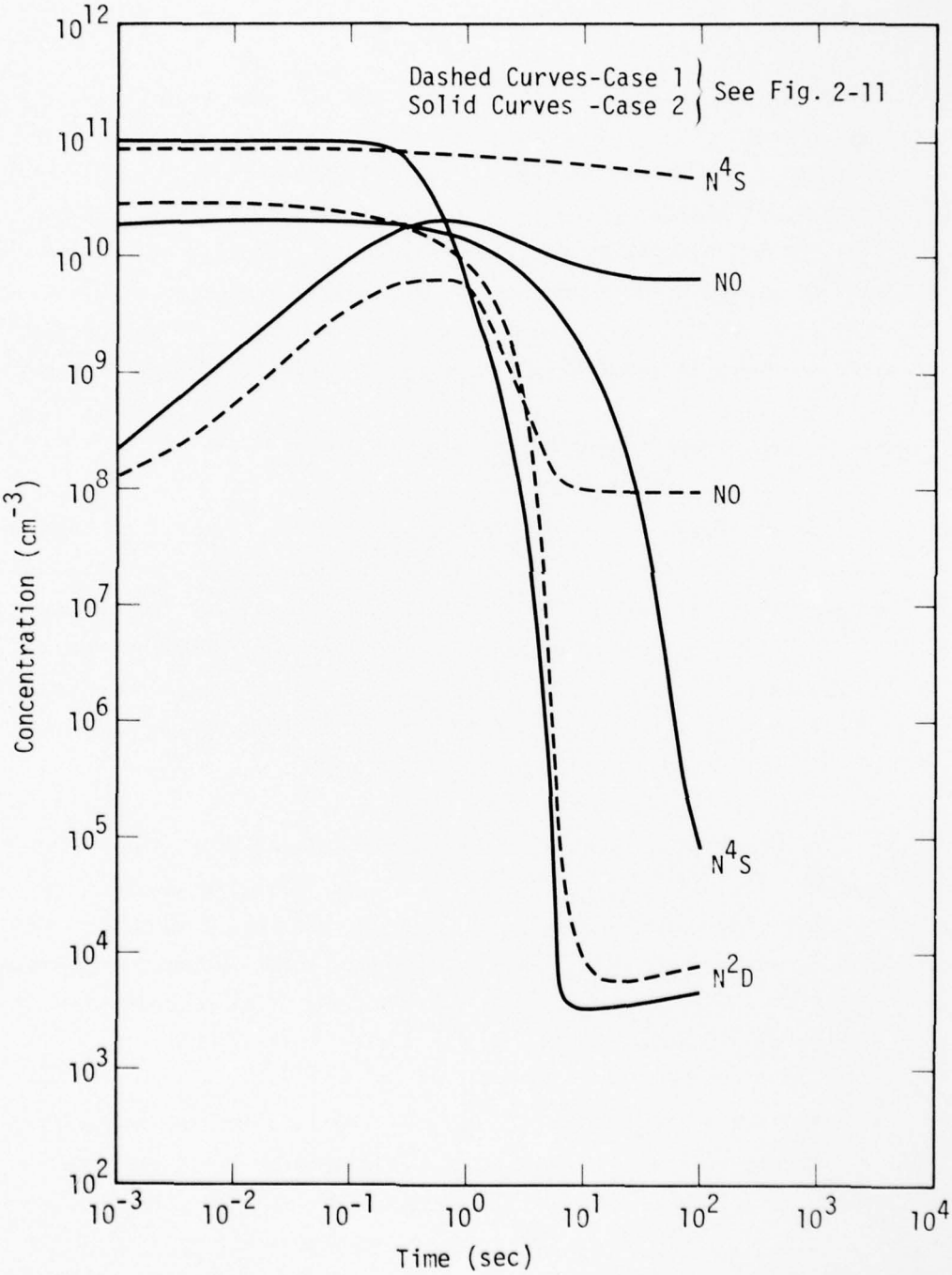

Figure 2-12. NO and N-atom concentrations at 110 km for two different combinations of $N(^4S)/N(^2D)$ branching ratios (T=500°K).

and by the initial photo-electron bombardment, can lead to greatly magnified errors in the calculated NO chemiluminescence at 5.4 and 2.7 μm and in the NO concentration. Errors in the NO concentration in turn produce additional errors in the calculated NO emission (especially the fundamental band near 5.4 μm) excited by the atom-interchange reaction $O' + NO \rightarrow O + NO'$. Although we assumed no hydro motion or temperature variation with time in our simplified calculations, there is no a priori reason to expect that inclusion of these effects would lead to significantly different conclusions.

Comments on Experimental Determination of f_1 and f_4

To determine f_1 and f_4 one would like, ideally, to bombard air in a chamber with a very short X-ray or electron (keV) pulse and then measure, as functions of time, the absorption of $N(^4S)$ and $N(^2D)$ resonance lines at 1200 Å and 1493 Å, respectively. The relative concentrations of $N(^4S)$ and $N(^2D)$, as functions of time, would thus be determined. The early-time results (prior to onset of electron-ion recombination) would yield f_4; the later-time results would yield f_1.

A method somewhat analagous to this was recently used by Kley, et al. (Reference 2-9) to measure the value of f_2 involved in NO^+ recombination. They used a flash lamp to ionize NO and a resonance lamp for emission of the 1200 Å and 1493 Å nitrogen lines. However, they were not faced with the problem of making measurements at very early times prior to the onset of recombination.

We have estimated the time scales involved for the measurements. If, for example, we assume a characteristic dimension of 10 cm for the bombardment volume, and require the resonance radiation to be attenuated by e^{-1} across it, then use of the reported resonance absorption cross section of $N(^4S)$ at 1200 Å leads to a requirement that $[N(^4S)] \gtrsim 5.6 \times 10^{11}$ cm^{-3} at 500 °K. This requirement implies a large initial electron density

(since about 2 electrons are produced for every $N(^4S)$ created) and leads to a half life for electron-ion recombination of only about 3 μsec. This would be the time available for making a determination of f_4. The later-time measurements to determine f_1 could presumably be carried out in a manner similar to that used by Kley et al., in which the number of nitrogen atoms produced promptly are distinguished from the number produced by dissociative recombination by using the SF_6 electron scavenger method.

SUMMARY AND RECOMMENDATIONS

We have examined certain aspects of the problem of predicting IR radiation from NO in a nuclear environment with a view to uncovering major areas of uncertainty. Crucial to such predictions, of course, are the excitation mechanisms themselves. The major ones are believed to be thermal collisions with NO and chemiluminescent reactions, particularly between atomic nitrogen and molecular oxygen. Certain auroral data suggest that thermal excitation of NO(v=1) by means of the atom-interchange reaction $O' + NO \rightarrow O + NO'$ is particularly efficient at high altitudes and may even dominate the chemiluminescent mechanism for excitation of the fundamental band in the aurora. Validation of the atom-interchange mechanism has important application to the overtone emission near 2.8 μm that may similarly be excited in large heated regions of a nuclear environment. We have sought to determine whether the existing field data (auroral) together with recent laboratory data on chemiluminescence, are sufficient to verify the respective roles of the two mechanisms.

A key element in the determination of both the thermal and the chemiluminescent contributions to IR emission from NO in a nuclear environment is the relative fraction of nitrogen atoms present in the ^4S and ^2D states. We have, therefore, also examined the various ways by which these atoms are made and have determined, by sensitivity studies, those branching ratios for which measurements are most needed.

Contrary to some of our earlier conclusions with respect to auroral data, the issue of atom-interchange versus chemiluminescent excitation of NO fundamental radiation no longer seems so clear, particularly when viewed in light of the data from rocket IC519.07-1B. Since this is an important issue to resolve, we hereby recommend a measurement program, preferably field and laboratory, with sufficient spectral resolution to provide unequivocal determination of the emitting species and bands. If successful, the planned field-widened interferometer experiment should be of great benefit in this regard. For complete verification of the thermal mechanisms, however, the field experiment should also include an independent determination of the NO and O concentrations, perhaps by use of a cryogenic neutral mass spectrometer. In addition, direct laboratory verification of the atom interchange mechanism, both with respect to the rate coefficient and the spectral distribution of emitted radiation at various temperatures, is needed.

With respect to NO chemiluminescence near 2.8 μm, theoretical calculations, that incorporate the recent COCHISE data on the $N(^2D) + O_2$ reaction, give values for the auroral emission that are lower than the aircraft and rocket data by factors of at least 2 to 3. Furthermore, certain nuclear data appear to be inconsistent with the conventional NO mechanism. Therefore, unless the 1978 DNA-AFGL auroral rocket program is able to definitely confirm the emitting specie(s) and excitation mechanisms involved, we recommend additional field programs be undertaken to resolve the apparent discrepancy.

Next, because of the sensitivity of NO chemistry and resulting emissions to uncertainties in branching ratios for production of $N(^4S)$ and $N(^2D)$ atoms, we recommend laboratory measurements to determine certain quantities f_1 and f_4. Here, f_1 is defined by the reaction

$$N_2^+ + e \rightarrow f_1 N(^4S) + (2-f_1) N(^2D) \quad ,$$

and f_4 is the fraction of nitrogen atoms produced in the ^4S state immediately following energy deposition by X rays or fast electrons. The remaining fraction, $(1-f_4)$, is usually assumed to be in the ^2D state although some atoms will certainly be left in the ^2P state as well. The fraction in ^2P is of interest, although with somewhat lower priority.

Quenching of the NO radiation becomes an important consideration at altitudes below about 110 km. Data on the quenching of NO(v=1) exist, but little exist for NO(v>1). However, our studies above show that the chemiluminescent emission rate is not particularly sensitive to the variation of the quenching rate with vibrational state v, at least for rates that vary no more strongly than linear with v. Of course it would be worth verifying experimentally what the variation with v actually is, but we presently assign a lower priority to this task.

In summary, we recommend the following measurement program, with the assigned relative priorities:

1. Auroral field measurements in the 5.0 - 6.5-μm and 2.6 - 3.2-μm regions with sufficient spectral resolution ($\lesssim 5$ cm^{-1}) to unambiguously identify the radiating species. (Priority 1)
2. Laboratory determination of the branching ratios for production of $N(^4S)$ and $N(^2D)$ atoms (a) by dissociative recombination in N_2^+ and, (b) immediately following energy deposition by X rays and β particles. (Priority 2)
3. Concurrent with 1, a measurement of the NO and O concentrations in the aurora. (Priority 3)
4. Laboratory confirmation of the rate constant for the reaction $O + NO' \rightarrow O' + NO(v>0)$ with spectral observation of the resulting emission over a wide temperature range. (Priority 3)
5. Laboratory determination of the quenching rates of NO(v>1) by O_2 and O. (Priority 4)

SECTION 3
OTHER EMISSIONS IN 2.6- TO 2.9-μm REGION

In addition to NO, other atmospheric molecules that can radiate in the wavelength region from about 2.6 to 2.9 μm include CO_2, H_2O, OH, HO_2, H_2O_2, HNO_2, and HNO_3. We have reviewed the potential significance of these species in a nuclear environment and discuss the conclusions in this section.

Except for CO_2, and for H_2O at low altitudes, these species are all very minor constituents of the ambient atmosphere. However, their potential importance in a nuclear environment lies in the possibility of their chemiluminescent formation (or vibraluminescent excitation in the case of CO_2) by the multitude of reactions that occur as the disturbed air returns to chemical equilibrium. With the exception of OH, the species listed are all polyatomics which are usually important only at and below the D region where 3-body reactions, or 2-body ones involving other polyatomics, are effective in their formation. Thus, although a low altitude favors the formation of these species, it also acts to depress the radiation from them because of collisional quenching.

We have used results of D-region chemistry benchmark calculations, performed with the code DCHEM, to estimate the relative formation rates of the species. (CO_2 is in a category by itself because its excitation by vibrational transfer from N_2 generally dominates that by chemiluminescent formation of the species.) The results show that the formation rate of H_2O_2, HNO_2, and HNO_3 are lower than those for OH and HO_2. Since the bands for all five species occur at about the same wavelength, we conclude that H_2O_2, HNO_2, and HNO_3 are relatively unimportant in this wavelength region.

As for H_2O, the dominant formation mechanisms involve reactions with complex hydrated water ions in which little exchange of energy occurs. Enhancements of the vibrational excitation of H_2O should, therefore, be minimal. For these reasons we dismiss from further consideration all species except CO_2, OH, and HO_2.

CO_2

Role In Nuclear Environment

A number of intercombination bands of CO_2 can contribute to radiation near 2.7 μm. The band strengths are probably known with sufficient accuracy so that the thermal emission from locally heated regions, especially those at lower altitudes where collision limiting is not important, can be calculated fairly well. At higher altitudes, above about 70 km or so where X rays from a high-altitude burst are deposited over large areas, there is the possibility of vibraluminescence persisting for long periods of time. This phenomenon is potentially important because it may degrade the performance of systems operating near 2.7 μm. Questions relating to the uncertainties involved in a determination of this emission will now be discussed.

Uncertainties

Figure 3-1 (from Reference 3-1) is a partial vibrational level diagram of CO_2 showing the origin of some of the intercombination bands near 2.7 μm. Also shown in Figure 3-1 is the relative position of the first few vibrational states of N_2. The close energy resonance between the 001 state of CO_2 and the $v = 1$ state of N_2 is responsible for the efficient conversion of N_2 vibrational energy into CO_2 radiation near 4.3 μm. However, excitation of the intercombination states that lie

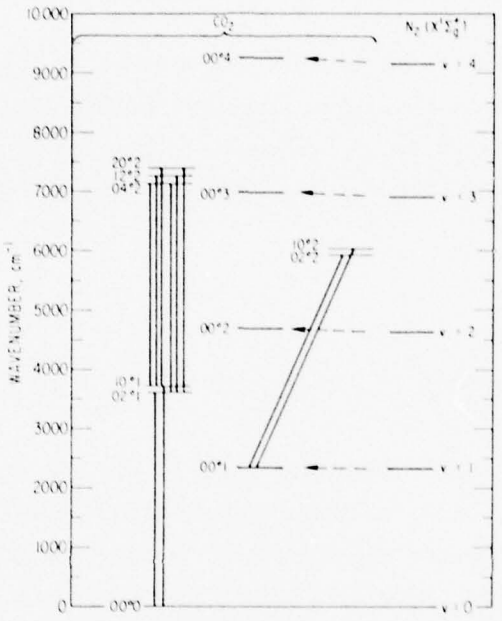

Figure 3-1. CO_2 - $N_2^{\ddagger}$ vibrational energy transfer and 2.7-μm emission bands.

above the 001 state can, presumably, come about either by transfer reactions such as

$$N_2(1) + CO_2(100) \rightarrow N_2(0) + CO_2(101) \qquad (3\text{-}1)$$

or, perhaps, by

$$N_2(v) + CO_2(000) \rightarrow N_2(0) + CO_2(00v) \qquad (3\text{-}2)$$

where the energy in $CO_2(00v)$ is partially redistributed, by collisions, among the other vibrational modes. For $v > 1$, Reaction 3-2 requires a multi quantum jump in both N_2 and CO_2 which, on theoretical grounds, should become increasingly less favored as Δv increases beyond unity. But details such as the rate of excitation by Reactions like 3-1 and 3-2, and vibrational redistribution and quenching are by no means well known. In fact, we are presently not in a good position to calculate the CO_2 vibraluminescence at 2.7 μm. The conventional wisdom is that the emission

should be relatively small (at least compared with that at 4.3 μm) because the branching ratios are believed to be such that transitions that emit at 4.3 μm are favored over those that emit at 2.7 μm by a factor of about 24 (Reference 3-2). For example, the states 101 and 021, shown in Figure 3-1, can decay by transitions to states 100 and 020, respectively, with emission near 4.3 μm, as well as by radiation to the ground state 000 (in the so-called "summation bands") shown in Figure 3-1. The Lockheed experiments (Reference 3-3) have not yet succeeded in confirming the assumed branching ratios for the 101 and 021 states, but it is hoped that the presently planned series of experiments involving laser excitation (Reference 3-4) will provide us with the required data for those states. Even so, there is still the question of branching ratios for the higher intercombination states that give rise to the so-called "difference bands", some of which are shown in Figure 3-1.

The potential importance of the CO_2 difference bands, indeed of CO_2 vibraluminescence at 2.7 μm in general, can be traced to experiments by Oettinger and Horn (Reference 3-1) in which the absolute intensity and spectral distribution of 2.7-μm radiation emitted from CO_2, after excitation by vibrational transfer from N_2, were measured. The apparatus involved a flow tube wherein ground-state CO_2 and vibrationally excited N_2 (excitation by an S-band generator) streams interacted to produce the CO_2 emission that was spectrally investigated at selected downstream positions. The results, compared with analytically derived counterparts for the summation bands, show that for an N_2 vibrational temperature of 1900°K, the difference bands at 2.7 μm contribute about 2.5 times as much as do the summation bands.

The information supplied in Reference 3-1 includes, besides the spectral intensity, the N_2 vibrational temperature, the N_2 pressure and the CO_2 partial pressure. From these data we have attempted to make a crude

estimate of the possible importance of CO_2 vibraluminescence at 2.7 μm relative to that at 4.3 μm. In the following we make no reference to specific vibrational states of N_2 and CO_2 but, rather, assume there are rate constants $k_{2.7}$ and $k_{4.3}$ such that

$$N_2^{\ddagger} + CO_2 \xrightarrow{k_{2.7}} N_2 + CO_2^{\ddagger} \xrightarrow{A_{2.7}} N_2 + CO_2 + h\nu_{2.7\ \mu m}$$

and

$$N_2^{\ddagger} + CO_2 \xrightarrow{k_{4.3}} N_2 + CO_2^{\ddagger} \xrightarrow{A_{4.3}} N_2 + CO_2 + h\nu_{4.3\ \mu m}$$

where $A_{2.7}$ and $A_{4.3}$ are Einstein coefficients for the 2.7- and 4.3-μm emissions, respectively. If $k_{2.7}^{(q)}$ and $k_{4.3}^{(q)}$ are the corresponding collisional quenching rate constants then, in steady state, the volume emission rates at 2.7 μm and 4.3 μm are given by

$$\dot{\Phi}_{2.7\ \mu m} = \frac{A_{2.7}k_{2.7}[CO_2][N_2^{\ddagger}]}{A_{2.7} + A_{4.3} + k_{2.7}^{(q)}[M]} \qquad (3\text{-}3)$$

$$\dot{\Phi}_{4.3\ \mu m} = \frac{A_{4.3}k_{4.3}[CO_2][N_2^{\ddagger}]}{A_{4.3} + k_{4.3}^{(q)}[M]} \qquad (3\text{-}4)$$

If $\Delta\ell$ is the path length across the interacting CO_2/N_2 streams, then the 2.7-μm intensity is

$$I_{2.7\ \mu m} = 5.8 \times 10^{-21}\ \dot{\Phi}_{2.7\ \mu m}\Delta\ell \quad (\text{watts cm}^{-2}\ \text{ster}^{-1}). \qquad (3\text{-}5)$$

If Equation 3-5 is equated to the measured intensity, we can then solve for the unknown excitation rate constant, $k_{2.7}$, provided values for the other parameters are supplied. The greatest uncertainty here is the effective quenching rate constant $k_{2.7}^{(q)}$. To be specific, we will assume that we can use the quenching rate measured by Finzi and Moore (Reference 3-5) for the 101 and 021 states, which gives us

$$k_{2.7}^{(q)} = 1.3 \times 10^{-10}[CO_2] \quad . \qquad (3\text{-}6)$$

Values for the Einstein coefficients $A_{2.7}$ and $A_{4.3}$ are about 15 sec^{-1} and 400 sec^{-1}, respectively (Reference 3-6). For the particular experimental arrangement where the total pressure $p = 1.1$ Torr, $P_{CO_2}/P = 0.043$, and the nitrogen vibrational temperature $T_{N_2} = 1720°K$, we find $[N_2] = 2.9 \times 10^{16}$ cm^{-3}, $[CO_2] = 1.2 \times 10^{15}$ cm^{-3}, and $[N_2^{\ddagger}] = 4.1 \times 10^{15}$ cm^{-3}. If we integrate in wavelength over the observed spectral intensity for this case we find

$$I_{2.7\ \mu m}(\text{measured}) \approx 4.5 \times 10^{-5}\ (\text{watts cm}^{-2}\ \text{ster}^{-1}) \quad . \quad (3\text{-}7)$$

Equating Equations 3-5 and 3-7, and using values for the parameters quoted above, along with $\Delta\ell \approx 2$ cm, we find

$$k_{2.7} \approx 8 \times 10^{-12}\ (\text{cm}^3\ \text{sec}^{-1}) \quad . \quad (3\text{-}8)$$

This is certainly a large rate constant for excitation of 2.7-μm vibraluminescence. In fact, it is about one order of magnitude larger than that for vibraluminescent excitation of 4.26 μm by the $N_2(1) \rightarrow CO_2(001)$ process. Of course, if we have overestimated the quenching, using Equation 3-6, then we have overestimated $k_{2.7}$ by a corresponding factor.

Nevertheless, if we do use the result 3-8, what is the implication for the aurora at altitudes above about 95 km where we can ignore the quenching? From Equations 3-3 and 3-4 we find, taking $k_{4.3} = 6 \times 10^{-13}$,

$$\frac{\dot{\phi}_{4.3\ \mu m}}{\dot{\phi}_{2.7\ \mu m}} \approx \frac{A_{4.3}}{A_{2.7}} \frac{k_{4.3}}{k_{2.7}} = 2.0 \quad (3\text{-}9)$$

This implies that for every two photons produced at 4.3 μm there is one produced at 2.7 μm. This is clearly too large an auroral emission rate at 2.7 μm even if we attribute all the observed 2.7-μm auroral emission to CO_2 instead of to NO. For example, for rocket A10.205-2, the observed 4.3 to 2.7 ratio varied from about 15 at 95-km altitude to 8 at 100 km and 2 at

110 km. Furthermore, the CVF auroral data peak at a wavelength of about 2.80 μm (in reasonable agreement with NO overtone chemiluminescence) whereas the CO_2 vibraluminescence, reported in Reference 3-1, peaks at about 2.70 μm. It is, therefore, unlikely that CO_2 is the principal contributor near 2.7 μm in the aurora.

The main purpose of the foregoing exercise, however, is to point out that in our present state of ignorance concerning vibraluminescent excitation of CO_2 radiation near 2.7 μm, arguments can be made to support emission rates that are not insignificant compared to those at 4.3 μm.

Recommendations

It would appear that there is a definite need for more laboratory measurements, perhaps along the lines of those by Oettinger and Horn, to determine the excitation and quenching rates necessary to clarify the role of CO_2 vibraluminescence near 2.7 μm so that, if significant, it can be modeled for use in codes such as ROSCOE. Specifically, we recommend a laboratory program designed to determine:

1. the CO_2 spectral intensity near 2.7 μm, compared with that at 4.3 μm, as a function of N_2 vibrational temperature. It is essential that the experiments be performed over a sufficiently broad pressure range to establish the effective quenching rate constants. (Priority 1)
2. if possible, the vibrational transfer rates from $N_2(v>1)$ to CO_2. (Priority 2).
3. branching ratios between 4.3 and 2.7 μm for the higher states of CO_2 that give rise to the difference bands near 2.7 μm. (Priority 2).

Tasks 2 and 3 should be done only if Task 1 shows that the 2.7-μm emission is significant under conditions of small or zero quenching.

OH

Role In Nuclear Environment

OH, with its fundamental band near 2.8 μm, is a very minor constituent of the ambient atmosphere. Consequently, thermal radiation from the species is not very significant. However, chemiluminescent excitation of OH, presumably through the reactions

$$H + O_3 \rightarrow OH(v \leq 9) + O_2 \qquad (3\text{-}10)$$

$$O + HO_2 \rightarrow OH(v \leq 6) + O_2 \quad , \qquad (3\text{-}11)$$

is responsible for one of the most intense airglow emissions at altitudes between about 80 and 90 km (see, for example, Reference 3-7). Direct enhancement of OH emission in auroras, however, is not observed (Reference 3-8).

In a nuclear environment, as in the ambient atmosphere, OH chemiluminescence should be insignificant above 100 km where the concentrations of the polyatomic reactants O_3 and HO_2 are small. Similarly, widespread enhancement in the concentrations of the atomic oxygen and hydrogen reactants, by X-ray absorption from high-altitude bursts, would not be expected much below about 45 km. There is, therefore, a limited altitude region, extending from perhaps 45 to 90 km, in which an increase in the concentrations of the reactants in Reactions 3-10 and 3-11 might occur to enhance the OH emission in a nuclear environment. However, with a quenching rate constant of 5×10^{-14} cm^3 sec^{-1}, inferred from airglow data (Reference 3-9), and an Einstein coefficient for the fundamental band of 34 sec^{-1}, collisional quenching sets in at altitudes below about 75 km thereby limiting the emission rate from the lower altitudes.

We have used the output from coupled hydro/chemistry-code calculations (MICE/IRCHEM) to infer the expected behavior of OH chemiluminescence

for two nuclear events: (i) Kingfish, and (ii) a high-yield burst at 200-km altitude. The results show that for altitudes below about 70 km the ozone concentration is enhanced over ambient values, but above 70 km it is decreased mainly because of destruction by reaction with atomic nitrogen. For both events we find that the OH intensity, arising from $H + O_3$ chemiluminescence, is depressed below pre-burst values because the negative contribution from altitudes above 70 km more than outweighs the positive contribution from the lower altitudes. This is true for both vertical and horizontal viewing directions.

Unfortunately, the MICE/IRCHEM calculations did not include the species HO_2 and so no estimates are available for the effect of Reaction 3-11 in these cases. However, chemistry benchmark calculations, using the DCHEM code, do show an increase in the O and HO_2 concentrations for at least tens of seconds after a burst although, for most altitudes and times, the formation rate of OH by Reaction 3-10 dominates that by Reaction 3-11. It seems unlikely, therefore, that in a nuclear environment the enhanced contribution to OH chemiluminescence from Reaction 3-11 is generally sufficient to offset the negative contribution from Reaction 3-10. Based upon the limited cases studied, we conclude that the OH intensity in a nuclear environment is generally suppressed below ambient values.

Uncertainties

Considerable work has been done in the laboratory (Reference 3-10), in the field (References 3-7, 3-11, 3-12), and through theoretical analyses (Reference 3-9) to account for the airglow data, mainly by Reaction 3-10. Less is known about OH excitation through Reaction 3-11. In particular, uncertainties exist with respect to:

1. the rate constant for Reaction 3-11
2. the initial vibrational distribution of OH following Reaction 3-11
3. the quenching of OH(v).

Recommendations

Before recommending any laboratory program to reduce the above-listed uncertainties, we feel that more code calculations should be done to definitely confirm our tentative conclusion that OH radiance is suppressed in a nuclear environment. To properly assess the relative importance of OH emission, such calculations should take due account of the NO overtone radiation excited by the atom-interchange reaction (see Section 2) and by chemiluminescence.

HO_2

Role In Nuclear Environment

HO_2 is also a very minor species in the ambient atmosphere. Like OH, its potential importance in a nuclear environment derives from the possibility of enhanced emission from its ν_1 fundamental band (near 2.9 μm) in chemiluminescent formation by reactions including, particularly,

$$OH + O_3 \rightarrow HO_2 + O_2 + 1.69 \text{ eV} \qquad (3\text{-}12)$$

and

$$H + O_2 + M \rightarrow HO_2 + M + 2.04 \text{ eV} \quad . \qquad (3\text{-}13)$$

To our knowledge, no direct observations of HO_2 chemiluminescence have been made. The possible importance of the species as an IR emitter is purely conjectural, based on formation rates calculated by D-region chemistry codes, especially DCHEM, run under nuclear-burst simulation conditions.

We have studied the results of DCHEM runs, as well as those from some code calculations performed for the natural OH airglow (Reference 3-9). Pertinent comments, as they pertain to the role of HO_2 in a nuclear environment, are as follows. First, for comparing the formation rates of OH and HO_2 by Reactions 3-10 and 3-12, respectively, we note that [OH] exceeds

[H] for altitudes up to about 60 km in the ambient atmosphere (Reference 3-9). At higher altitudes the [OH]/[H] ratio drops rapidly so that at 100 km it is about 10^{-6}. Second, the rate constant for HO_2 formation by Reaction 3-12 is about 2 orders of magnitude smaller than that for formation of OH by Reaction 3-10. Third, under nuclear-burst conditions, [OH] builds up for some tens of seconds at altitudes below about 70 km as does also $[O_3]$ provided the initial fractional ionization is sufficiently high. Fourth, as discussed above, $[O_3]$ is generally depressed below ambient values above about 70 km. The overall result is that the HO_2 formation rate by Reaction 3-12, and hence also the HO_2 chemiluminescence, is enhanced below 70 km. In certain time-altitude regimes, the formation rate of HO_2 even exceeds that of OH. However, because of the rapid decay of [OH] with increasing altitude above 70 km, there will not be a large contribution to HO_2 emission at the higher altitudes as there is for OH emission. Since the DCHEM results show that the formation rate of HO_2, even at the lower altitudes, is not significantly greater than that for OH, we would expect that the HO_2 intensity along any sight path, which of necessity includes contributions from high altitudes, would be less than that for OH.

These semi-qualitative arguments lead one to the conclusion that the intensity of HO_2 chemiluminescence is probably on the same order as, or smaller than, that of OH chemiluminescence which, as we have seen above, appears to be depressed below normal airglow levels in a nuclear environment. As to the wavelength positions of the two emissions, we know that the wavelength of the (100-000) band of HO_2 lies about 0.1 μm to the red side of the (1,0) band of OH. However, the reactions forming OH are more exothermic than those forming HO_2 and so the OH should be populated to higher vibrational states than the HO_2. Thus, the peak in the chemiluminescent spectrum of OH would be shifted more to the red side of its (1,0) band than would be the case for HO_2 with the result that the two spectral distributions should largely overlap.

Uncertainties

Apart from some uncertainty in the rate coefficients for Reactions 3-12 and 3-13, the major uncertainties associated with modeling the HO_2 emission in a nuclear environment are:

1. the vibrational distribution of HO_2 following its formation by Reactions 3-12 and 3-13
2. the quenching rates for $HO_2(v,00)$
3. the band strength for the ν_1 fundamental which is needed for a good description of the quenching factor.

Recommendations

No experiments on HO_2 are recommended at this time. However, more code calculations should probably be done to verify the tentative conclusions reached above and to determine the magnitude of the intensity along tangent and zenith paths for the case of at least one high-yield, high-altitude burst. Such a calculation should include, for comparison, the OH and NO contributions near 2.8 μm.

SECTION 4
EMISSION IN 4.1- TO 4.6-μm REGION

Background radiation from about 4.1 to 4.6 μm, induced by atmospheric nuclear explosions, may degrade the performance of systems designed to operate in this wavelength region. Potential radiators include CO_2(4.3 μm), CO(4.6 μm), $N^{14}N^{15}$(4.4 μm), NO^+(4.3 μm), and N_2O(4.5 μm). We have addressed the problem of determining the relative importance of these species in a nuclear environment, and the principal uncertainties associated with modeling their emissions. For this purpose, we have made use of prior calculations, including chemistry benchmark runs and output from large MHD codes and, where possible, have utilized auroral field data. The results of this effort are summarized in this section. They are presented in order of the species listed above.

CO_2

Carbon dioxide is the dominant emitter in this wavelength band, and the one most studied by the weapon effects community. The reason, of course, is because of its relatively high mixing ratio in the ambient atmosphere, coupled with the fact that $N_2(v=1)$, which is initially the sink for about 5 percent of the X-ray energy released from a nuclear detonation, can readily transfer its energy to CO_2 which then radiates at 4.3 μm (and other bands) over a long period of time. In the past few years a lot of effort has gone into modeling this emission. More recently, refinements have been added to allow for radiation trapping of the 4.26μm resonance radiation below about 100 km, for emission by the so-called weak isotopic and hot bands, and for fluorescence resulting from absorption by CO_2 of sunlight and bomb-light at 2.7 μm with subsequent reradiation in other bands, especially those

near 4.3 μm. The basic theory of CO_2 vibraluminescence near 4.3 μm is substantiated by the ICECAP auroral measurements, which in turn have served to refine the theory. The recent SPIRE (spectral infrared experiment) experiment in Alaska obtained useful data for the purpose of confirming the fluorescence mechanism. Much of the theoretical and laboratory work on CO_2, which is still ongoing, has been done by Kumer and James (see, for example, References 3-2, 3-3, and 4-1 to 4-3) who have also emphasized the areas where more measurements are required to improve the accuracy of our prediction capability. Since these requirements are well known to DNA, it seems redundant to repeat them here other than to add, perhaps, the need for measurements of the CO_2 mixing ratio above 100 km. For this reason we pass on to a consideration of the other species.

CO

Role In Nuclear Environment

Carbon monoxide, with its fundamental band near 4.7 μm, is a very minor constituent of the ambient atmosphere with a measured mixing ratio up to 50 km of about 1×10^{-7}, which is less than 1/3000 that of CO_2. It has potential importance in a nuclear environment only because it can be formed by dissociation of CO_2 in low- and intermediate-altitude fireballs and then carried aloft in the subsequent fireball rise. Because of its high dissociation energy, and non-reactive character, the species should have a long life at the higher altitudes where it can presumably be excited by resonant scatter of solar and/or earthshine photons.

Detailed fireball calculations, performed for chemistry benchmark purposes (using the FIRECHEM code at MRC), have shown that, although the CO content of low-altitude fireballs may exceed that of CO_2 by several orders of magnitude for a few seconds, the CO_2 concentration generally builds up again, partly by entrainment of ambient CO_2 and partly at the expense of

the CO, so that by the time the fireball has risen a few scale heights, the CO_2 is again dominant. This fact would appear to rule out long term excitation of the CO by vibrational transfer from N_2 which will tend to excite the more abundant CO_2. An exception to this rule may occur for high-yield bursts, such as Teak, detonated above 60 km or so, for which little or no entrainment is believed to occur and not much reformation of the CO_2 is expected.

In summary, it appears that an appreciable amount of CO may be formed in low- and intermediate-altitude fireballs and lofted to altitudes of 100 km or more where it will have a long life against chemical destruction although its concentration will be diluted by diffusion and other transport processes. The dominant excitation mechanism, when thermal collisions are no longer important, is likely to be earthshine scatter.

Uncertainties

The impact on systems operating in this spectral region will depend on the details of the nuclear bursts and the CO concentrations present. Given the concentrations, however, prediction of the infrared intensity from CO should not entail much uncertainty since the band strength is well known. The greatest uncertainty lies in the determination of species concentrations which depends on fireball phenomenology. Entrainment and mixing of ambient air are quite crucial in this determination, but these phenomenon are only poorly understood.

Recommendations

We do not recommend any optical or other measurements relative to CO at this time.

$N^{14}N^{15}$

The $N^{14}N^{15}$ molecule, existing in the atmosphere with a relative abundance of 0.72 percent, is expected, on theoretical grounds, to radiate in its fundamental vibration-rotation band at 4.36 μm. As reported by Garstang (Reference 4-4), Bates and Poots (Reference 4-5), utilizing a formulation of Wu (Reference 4-6), calculated a value for the Einstein transition probability, A_{10}, for the fundamental band of the ion $(N^{14}N^{15})^+$ of 2×10^{-2} sec^{-1}. This value has been assumed in the Russian literature (Reference 4-7) to apply, approximately, to the netural species also. For purposes of determining the possible importance of the species in a nuclear environment, we too shall adopt that value, although clearly, until measurements are made, it must be assumed to be only an order-of-magnitude estimate.

Role In Nuclear Environment

As Kennealy (Reference 4-8) has pointed out, use of the above value for A_{10} leads to a volume emission rate at 4.36 μm, from $N^{14}N^{15}$, that should dominate that at 4.26 μm, from CO_2 vibraluminescence, in the altitude region above about 110 km. This is because the $N^{14}N^{15}$ emission rate is proportional to $[N_2(v=1)]$ whereas the CO_2 vibraluminescence involves $[CO_2]$ as an additional factor which, other things being equal, causes it to decrease faster with increasing altitude than the $N^{14}N^{15}$ emission rate. The main question, however, is whether or not the emission intensity at these altitudes is significant enough to worry about. We have addressed this question by calculating the expected zenith intensity for the case of a high-yield burst at 200-km altitude using the species concentrations and the nitrogen vibrational temperature output by the MHD code MICE. Our results give the thermal emission from the (1,0) band of $N^{14}N^{15}$ at 4.36 μm and also, for comparison, the vibraluminescence from the 4.26-μm band of CO_2.

For emission from $N^{14}N^{15}$ we have used the relations

$$\dot{\Phi}^{N^{14}N^{15}}_{4.36\ \mu m} = \delta A_{10}[N^{14}N^{15}(1)] \quad \text{(photons cm}^{-3}\ \text{sec}^{-1}\text{)}$$

$$= \alpha\delta A_{10}[N_2(1)]$$

$$= \alpha\delta A_{10}[N_2](1-e^{-3291/T_V})e^{-3291/T_V} \quad . \qquad (4\text{-}1)$$

Here, α is the relative abundance of $N^{14}N^{15}(7.2\times10^{-3})$, T_V is the nitrogen vibrational temperature, and δ is the collision limiting factor that allows for the fact that at the higher altitudes thermal equilibrium among vibrational states does not prevail because collisional excitation cannot compete with deexcitation by radiation. For δ we have adopted the expression

$$\delta = \frac{\nu'_{10}}{A_{10} + \nu'_{10}} \qquad (4\text{-}2)$$

where the collisional deexcitation rate, ν'_{10}, of $N^{14}N^{15}(1)$ is assumed to be controlled by V-V exchange with N_2 and by V-T collisions with atomic oxygen. Values for ν'_{10} were calculated using the equation

$$\nu'_{10} = 10^{-17}T^{1.5}e^{91.5/T}[N_2] + 2.47\times10^{-22}T^{2.87}[O] \quad (\text{sec}^{-1}) \quad . \qquad (4\text{-}3)$$

A_{10} is assumed equal to 0.02.

For temperatures above about 1000°K, collisional excitation of $N^{14}N^{15}$ to vibrational states higher than $v = 1$ will begin to occur so that contributions from bands (2,1), (3,2), etc., should also be included. Equation 4-1 can be corrected for this by multiplying by the factor $(1-e^{-3291/T_V})^{-2}$. At 5000°K this factor is 4.3; at 10,000°K it is 12.7.

For CO_2 vibraluminescence above 100-km altitude, it is sufficient to adopt the simple relation

$$\dot{\Phi}^{CO_2}_{4.26\ \mu m} = k[CO_2][N_2(1)] \tag{4-4}$$

based on the scheme

$$N_2(1) + CO_2(000) \xrightarrow{k} N_2(0) + CO_2(001) \tag{4-5}$$

$$CO_2(001) \longrightarrow CO_2(000) + h\nu_{4.26\ \mu m} \tag{4-6}$$

where the rate constant, k, can be approximated as

$$k = \text{Min} \left\{ \begin{matrix} 8 \times 10^{-11} \\ 10^{-12} e^{-0.0019T} + 1.7 e^{0.0022T} \end{matrix} \right\} . \tag{4-7}$$

The results of the calculations are shown in Figures 4-1 through 4-5. They include post-detonation times from 60 to 600 sec and zenith intensities at 200- and 400-km range from ground zero. Figures 4-1 through 4-4 show the zenith intensity profiles along the two vertical paths at selected times after burst. In these figures, the intensities are given in megarayleighs (10^{12} photons cm^{-2} sec^{-1}). They can be converted to units of watts cm^{-2} $ster^{-1}$ by multiplying by 3.6×10^{-9}. Figure 4-5 presents the results in a different form; namely, the intensities as functions of time at three different altitudes.

The detailed behavior of some of the curves shown in these figures may seem peculiar but, basically, it stems from the hydro motion of the region that transports air of varying temperatures across the two chosen vertical sight paths. In any event, the results do show that the zenith intensity from $N^{14}N^{15}$ dominates that from CO_2 by factors of roughly 3.5 at 120-km altitude, 20 at 160 km, and 30 at 200 km. As to the total intensity,

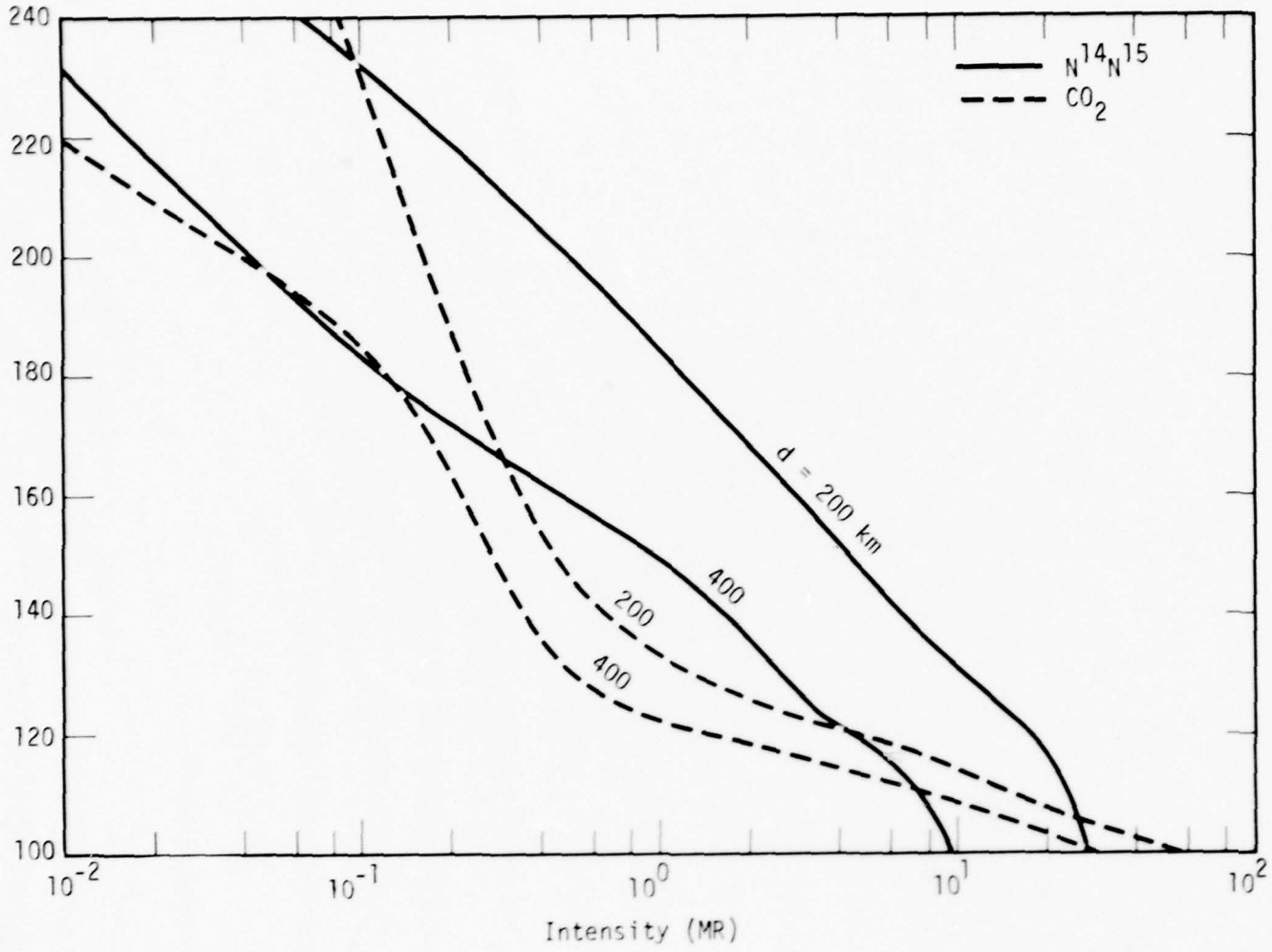

Figure 4-1. Calculated zenith intensity in 4.3-μm band from $N^{14}N^{15}$ (thermal) and CO_2 (vibraluminescence) at two horizontal ranges, d, from ground zero of a high-yield burst at 200-km altitude (time = 60 sec).

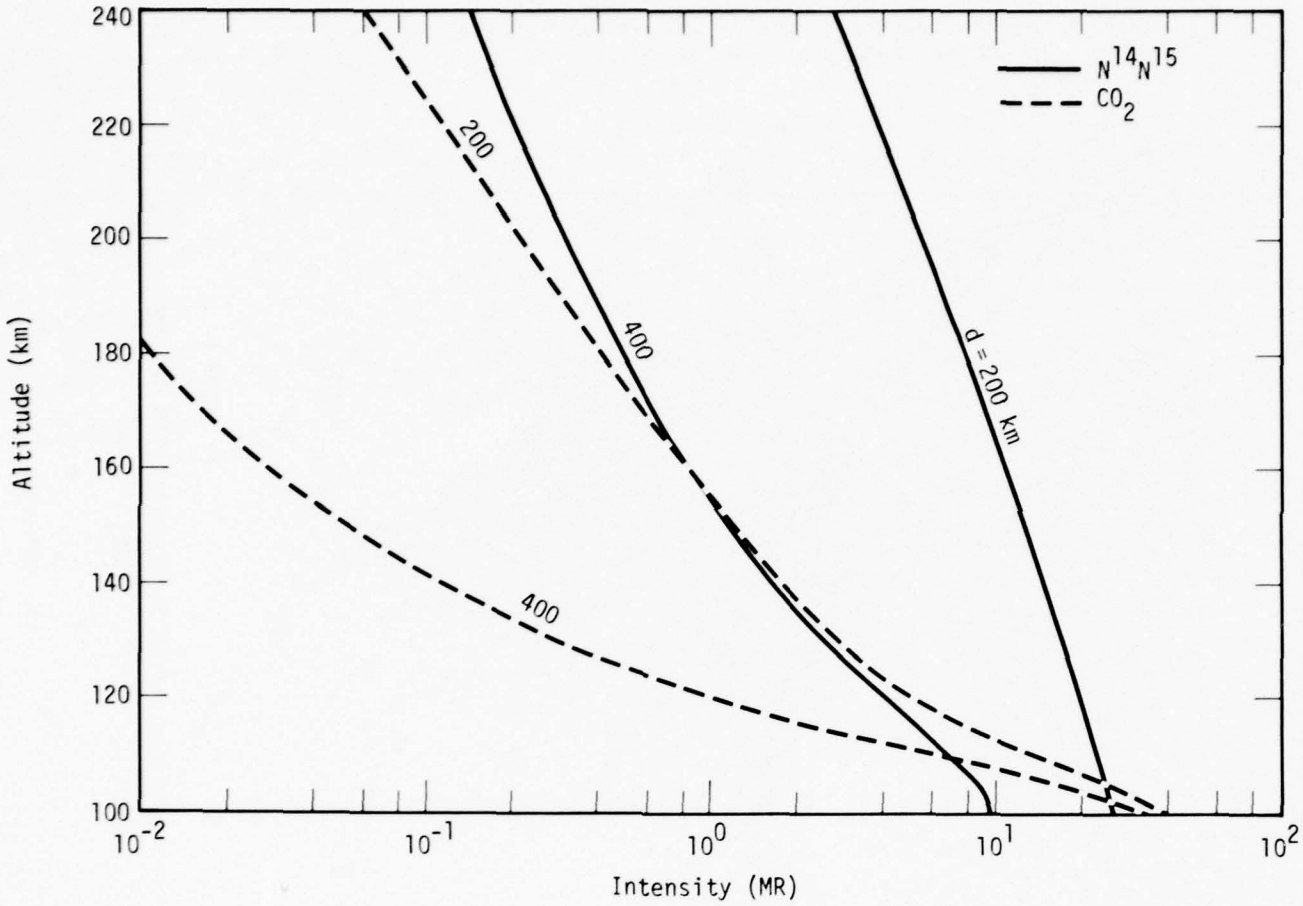

Figure 4-2. Calculated zenith intensity in 4.3-μm band from $N^{14}N^{15}$ (thermal) and CO_2 (vibraluminescence) at two horizontal ranges, d, from ground zero of a high-yield burst at 200-km altitude (time = 150 sec).

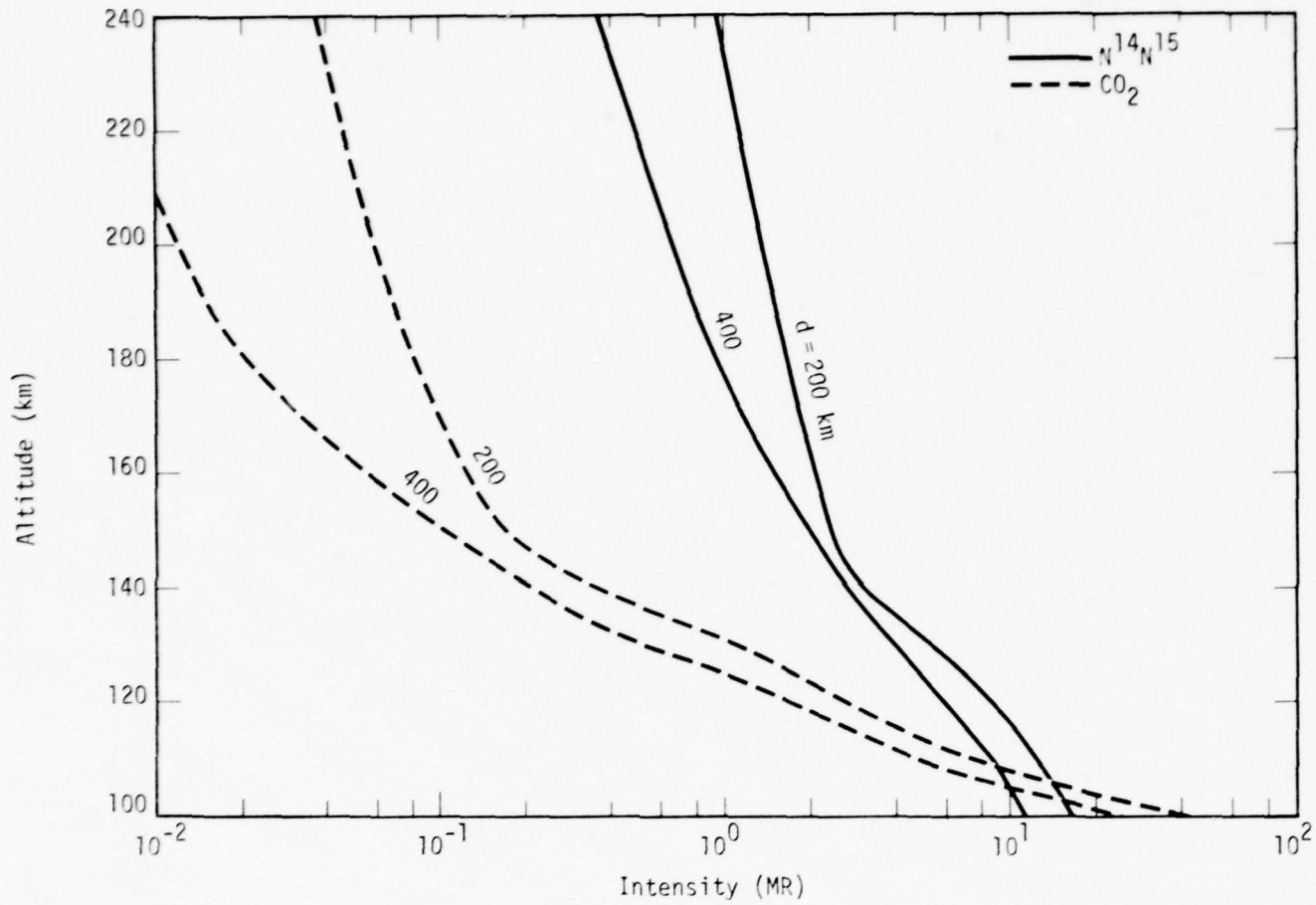

Figure 4-3. Calculated zenith intensity in 4.3-μm band from $N^{14}N^{15}$ (thermal) and CO_2 (vibraluminescence) at two horizontal ranges, d, from ground zero of a high-yield burst at 200-km altitude (time = 300 sec).

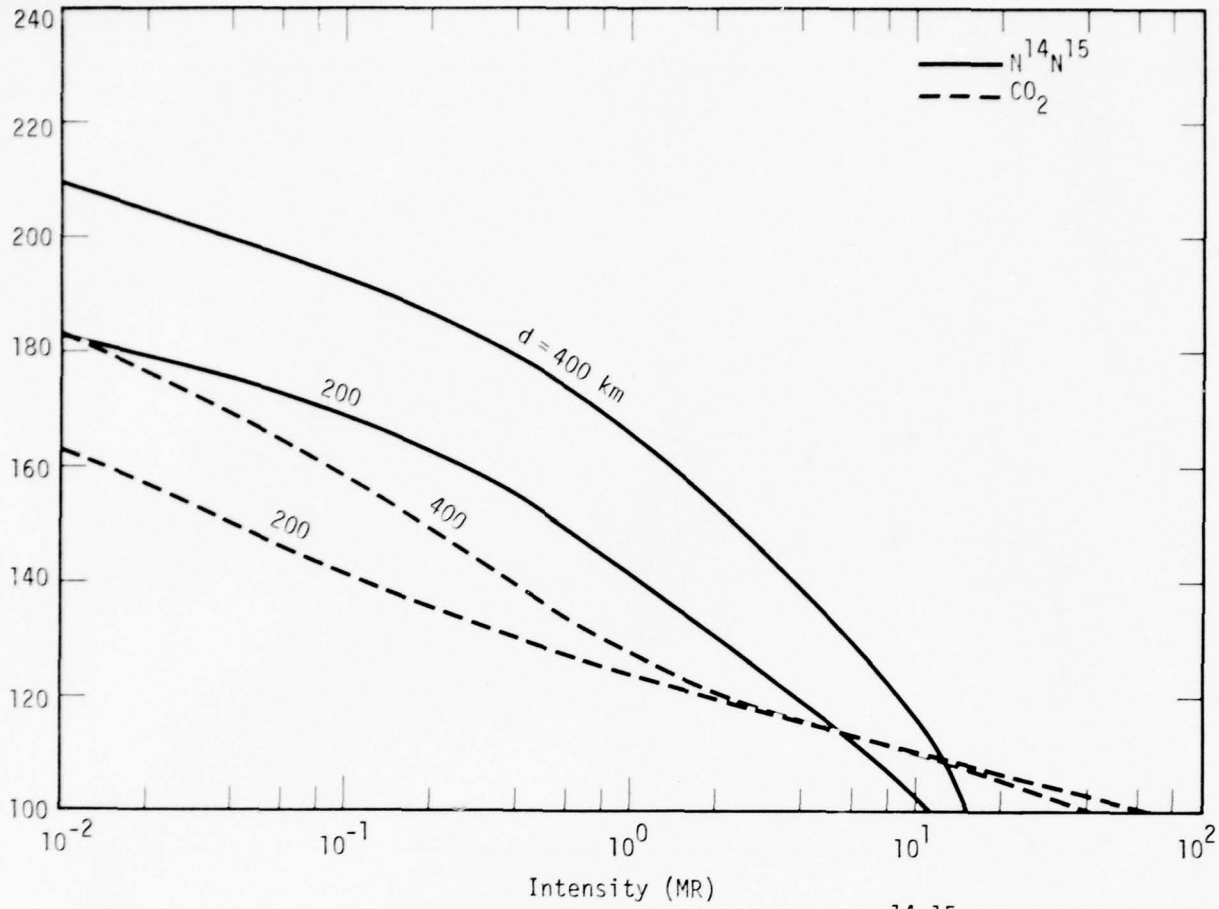

Figure 4-4. Calculated zenith intensity in 4.3-μm band from $N^{14}N^{15}$ (thermal) and CO_2 (vibraluminescence) at two horizontal ranges, d, from ground zero of a high-yield burst at 200-km altitude (time = 600 sec).

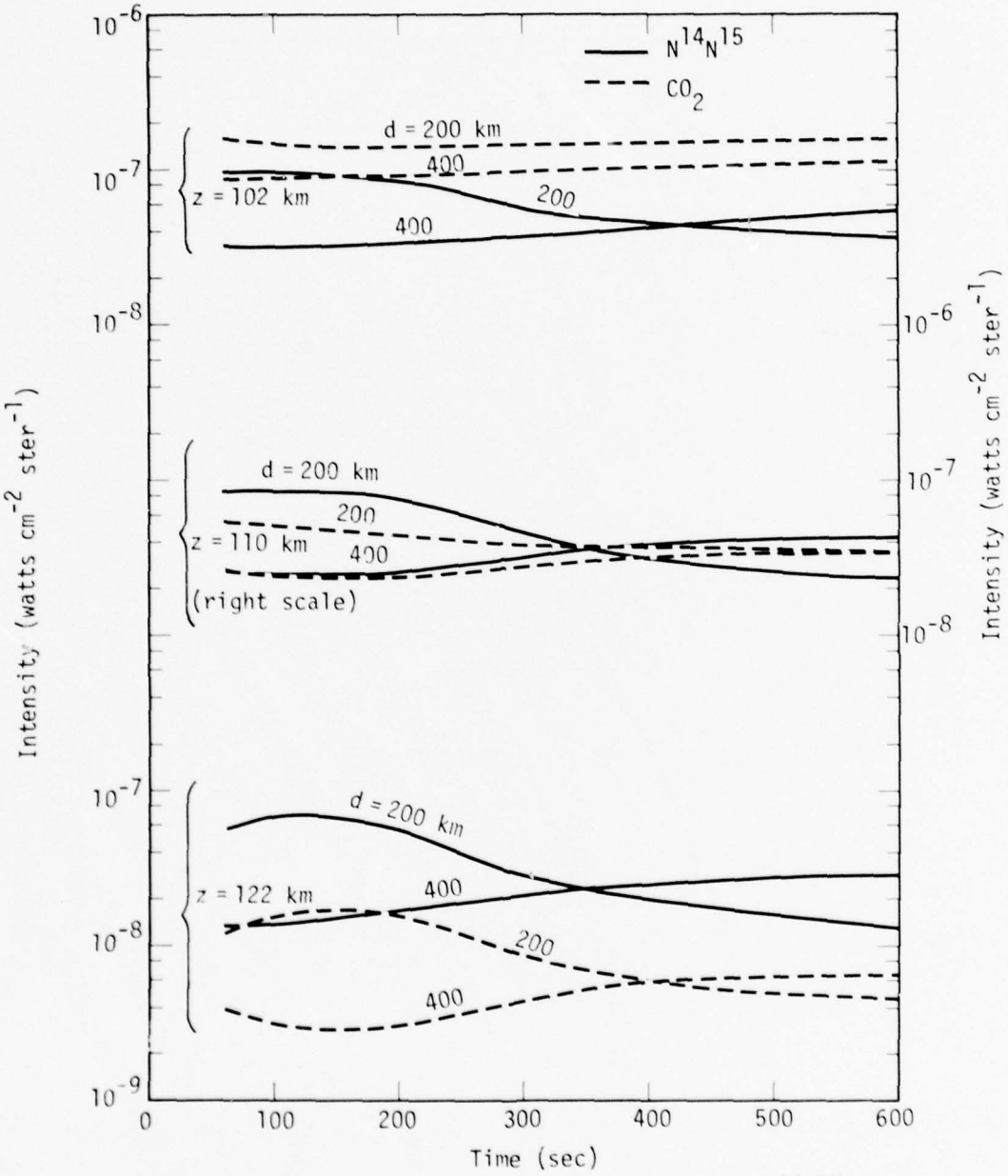

Figure 4-5. Calculated zenith intensity in 4.3-μm band from $N^{14}N^{15}$ (thermal) and CO_2 (vibraluminescence) at three altitudes, z, and at two horizontal ranges, d, from ground zero of a high-yield burst at 200-km altitude.

Figure 4-5 shows a zenith value at 122-km altitude, 400 km range from ground zero, as great as 3×10^{-8} watts cm^{-2} $ster^{-1}$ in the (1,0) band of $N^{14}N^{15}$ even 10 minutes after the burst. Contributions from the other fundamental bands (2,1) (3,2), etc., will, as mentioned above, make the numbers even larger.

These results show quite clearly the potential importance of $N^{14}N^{15}$ in a nuclear environment, especially if the band strength for the fundamental is as large as we have assumed.

Consideration Of Low-Altitude Effects

Another question relating to $N^{14}N^{15}$ that we have addressed is the potential importance of the molecule at altitudes below about 90 km in acting as an escape route for the trapped 4.26-μm CO_2 resonance radiation. If, as we have assumed, the radiative lifetime of $N^{14}N^{15}(v=1)$ is 1/.02 = 50 sec, then this is short compared with the 8 minute lifetime (Reference 4-2) for decay of N_2 vibrational quanta by transfer to and radiation from CO_2 at 80-km altitude.

In considering what happens to a vibrational quanta of $N^{14}N^{15}$, however, it is necessary to allow for vibrational exchange with N_2 that should be rapid at the lower altitudes because the $v = 1$ states of the two isotopes are within 39 cm^{-1} of perfect energy resonance. In fact, assuming the rate constant for vibrational exchange between the two isotopes is the same as that between N_2 and $N_2(v=1)$, which is about 3×10^{-13} cm^3 sec^{-1} (Reference 4-9), then over 4×10^3 exchanges with N_2 would occur before one quanta is lost by $N^{14}N^{15}$ in radiation. If we ignore CO_2 and assume that the only way an $N_2(v=1)$ quanta can be lost permanently is by transfer to and

radiation from $N^{14}N^{15}$, then solution of the simple set of reactions

$$N_2(1) + N^{14}N^{15}(0) \longrightarrow N_2(0) + N^{14}N^{15}(1)$$

$$N^{14}N^{15}(1) \xrightarrow{A_{10}} N^{14}N^{15}(0) + h\nu_{4.36\ \mu m}$$

leads to the approximate result

$$[N_2(1)] \approx [N_2(1)]_o e^{-\alpha A_{10} t} \qquad (4\text{-}8)$$

where, again, α is the relative abundance of $N^{14}N^{15}$. For values of α and A_{10} of 7.2×10^{-3} and 2×10^{-2}, respectively, this leads to an effective decay time, $(\alpha A_{10})^{-1}$, for $N_2(1)$ (and for $N^{14}N^{15}(1)$) of 1.93 hours at all altitudes below 100 km. Since this is much longer than the decay time of $N_2(1)$ in the presence of CO_2, we conclude that the presence of $N^{14}N^{15}$ will not alter the decay rate of $N_2(1)$ nor the emission rate from CO_2. In fact, most of the vibrational energy initially deposited in $N^{14}N^{15}$ below about 100-km altitude should eventually be radiated, not by $N^{14}N^{15}$, but by CO_2, either through diffusion of the trapped resonance radiation at 4.26 μm or through the weak isotopic and hot bands.

Uncertainties

The major uncertainty lies in the band strength (alternatively, the Einstein A coefficient) for the fundamental. An order of magnitude decrease in the value assumed here would render the species of marginal importance. Uncertainty also exists with respect to deexcitation of the vibrational states by V-V exchange with N_2 and by V-T collisions with atomic oxygen. Information on the quenching is needed for proper inclusion of the collision limiting at altitudes where $N^{14}N^{15}$ if likely to be important.

Recommendations

It is recommended that measurements be made to determine:

1. the band strength for the fundamental of $N^{14}N^{15}$ (Priority 1)
2. the vibrational exchange rate between N_2 and $N^{14}N^{15}$ and also the quenching rate of $N^{14}N^{15}(v)$ by atomic oxygen (Priority 2).

NO^+

Role In Nuclear Environment

The potential importance of NO^+ as a radiator near 4.3 μm in a nuclear environment stems from the fact that its excitation should occur mainly through chemiluminescent reactions that are energetically capable of populating high vibrational states of the ion. Thus, emission from (v,v-1) bands, extending into wavelength regions that overlap the so-called red spike region of CO_2, might be expected to have some systems impact.

The reactions

$$N_2^+ + O \longrightarrow N + NO^+ \qquad (4\text{-}9)$$

$$O_2^+ + NO \longrightarrow O_2 + NO^+ \qquad (4\text{-}10)$$

$$N^+ + O_2 \longrightarrow O + NO^+ \qquad (4\text{-}11)$$

$$O_2^+ + N \longrightarrow O + NO^+ \qquad (4\text{-}12)$$

$$O^+ + N_2 \longrightarrow N + NO^+ \qquad (4\text{-}13)$$

are all sufficiently exothermic to form NO^+ in vibrationally excited states. However, following prompt energy deposition, these reactions are over with in a few seconds except at altitudes above about 150 km or so where the formation rate and, therefore emission rate of NO^+ tends to be low. For example, for the case of the high-yield burst at 200-km altitude considered above (see discussion under $N^{14}N^{15}$), we find that for a post detonation

time of 60 sec the estimated volume emission rate from NO^+ at 130-km altitude is about one order of magnitude less than that from CO_2 vibraluminescence and nearly two orders less than our estimate of the $N^{14}N^{15}$ contribution. At 200-km altitude, emission from the three species is about comparable, but the intensities are so low there as to have little systems impact. Thus, in terms of prompt deposition effects, we would expect significant NO^+ intensities for only a few (perhaps 10 or 20)seconds after a single high-altitude burst, although in a multiburst environment the effects could persist much longer.

On a longer term basis, there is the possibility of NO^+ chemiluminescence at lower altitudes due to energy deposition by delayed beta and gamma radiation from the debris region. To quantify this emission, we considered the case of a 1-MT fission-yield burst at 300-km altitude, 100 sec after the burst, with a debris radius of 500 km. From the results presented in Reference 4-10, we first calculated the electron production rate due to delayed β and γ deposition along a vertical path below the debris region. Next, from results of previous ARCTIC code calculations and D-region benchmark chemistry calculations, we determined that, in the absence of quenching, approximately one NO^+ photon is expected per ion pair created. Then, applying the rate constant for quenching $NO^+(v=1)$ by N_2 measured by Bien (Reference 4-11), we calculated the zenith intensity as a function of altitude. The results show that for altitudes up to about 60 km, which is where the energy deposition peaks, the zenith intensity is constant at about 6×10^{-11} watts cm^{-2} $ster^{-1}$ and then decreases with altitude to a value of about 6×10^{-12} at 100 km. Larger values will attain at earlier times, smaller ones at later times. The smallness of these numbers is due to the severe quenching of the radiation which amounts to a factor of 10^{-5} at 60 km and 10^{-4} at 40 km.

In spite of the smallness of these numbers, two factors may operate to make NO^+ not entirely uninteresting from the systems point of view. One

is the fact that the emission arising from the beta deposition is probably structured, which means that smaller backgrounds are required to interfere with scanning systems; the other is the possibility that the quenching is much less severe for the higher vibrational states of NO^+ because the energy resonance with N_2 becomes increasingly worse for values of $v \geq 2$. Thus, the (3,2), (4,3), etc. hot bands may appear relatively stronger than do the (1,0) and (2,1) bands.

In summary, it would appear that NO^+ does not have a spectacular IR role to play in a nuclear environment, partly because the high-altitude excitation mechanism (chemiluminescence) is rather short lived, and partly because the low-altitude fluorescence/chemiluminescence from β and γ deposition is severely quenched. However, because of the possibility of continuing excitation at high altitude in a multiburst environment, and the possibility that the hot bands of the fundamental may suffer relatively less quenching at the low altitudes, it is still worthwhile to model the emission for potential systems application and to try to improve our prediction capability.

Uncertainties

The main uncertainties that presently exist with respect to calculation of the NO^+ emission are as follows:

1. The vibrational distribution of NO^+ immediately following Reactions 4-9 through 4-13 is totally unknown. The usual assumption of equal population of the levels up to the maximum allowed by energy conservation may be quite wrong and lead to gross errors in the photon efficiency and the spectral distribution of the radiation.

2. The quenching by N_2 of the vibrational states for $v > 3$ is not known.

3. The Einstein A coefficients are incompletely known. Theoretical work by Billingsley (Reference 4-12) has given values for $A_{1,0}$ and $A_{2,1}$, but the experimental values obtained by Bien (Reference 4-11) are nearly 2.5 times larger. The A coefficients are necessary for the purpose of determining the quenching factors to apply to the NO^+ chemiluminescence.

To our knowledge, no one has positively identified NO^+ as the source of any of the IR radiation observed under aurorally disturbed conditions. Comparisons between calculations and field data at 4.3 μm can usually be explained on the basis of CO_2 vibraluminescence (see, for example, References 2-3 and 4-2). The intensity, the shape of the main spectral feature at 4.3 μm (observed with low resolution CVF spectrometers), and the decay time of the radiation are in most cases consistent with the CO_2 mechanism. However, we do find that the calculated NO^+ contribution at 4.3 μm, relative to that from CO_2, is rather sensitive to the spectral hardness of the incident auroral electron flux. In fact, for one event in the ICECAP series ('75 Multi, rocket IC519.07-1B), our calculated contribution to the 4.3-μm radiance is an appreciable fraction of the total amount observed, and it appears to give, when combined with the CO_2 contribution, better agreement* with the data at 110 km on rocket ascent than does the calculated CO_2 radiance alone. Also, the CVF data do show emission on the long wavelength side of the main CO_2 feature at 4.3 μm, part of which may arise from the (v,v-1) bands of the NO^+ fundamental system. Not until data are taken with higher resolution, however, will we be able to positively identify the source of the auroral emissions.

* We refer here to Reference 2-3, Figure 2-15 and to later work, not published, in which the ARCTIC code results have been modified to reflect Bien's measured quenching rate and have also been reduced to bring the measured and calculated 3914-Å intensities into line.

Recommendations

We recommend a measurement program to determine:

1. the initial vibrational distribution of the NO^+ formed by Reactions 4-9 through 4-13 (Priority 1).

Selection of the most important of these reactions is difficult. At high altitudes the molecular ions will disappear rapidly by dissociative recombination leaving mainly Reactions 4-11 and 4-13. However, at low altitudes, in the β patch, the other reactions, with the possible exception of 4-12, are also significant.

2. the quenching rate of $NO^+(v)$ for $v > 3$ (Priority 2).

3. the Einstein A coefficients with better accuracy (Priority 3).

N_2O

Role In Nuclear Environment

Nitrous oxide, with its ν_3 fundamental band at 4.5 μm, is a very minor constituent of the ambient atmosphere with a measured mixing ratio that decreases with increasing altitude from a value of about 3×10^{-7} at 10 km to 1×10^{-7} at 30 km. The potential importance of the species lies in the position of its ν_3 band to the red side of the ν_3 fundamental of CO_2 and the possibility of its enhancement in a nuclear environment. Historically, however, the species has not been considered very interesting from the nuclear IR point of view for several reasons. With a dissociation energy (+ activation energy) of just over 2 eV, it is destroyed at relatively low temperatures in fireballs, and so thermal emission from it is quite low. Outside fireballs, the major formation reaction is usually considered to be $N + NO_2 \rightarrow N_2O + O$ where the NO_2 comes mainly from reaction of NO with odd

oxygen. But, by the time NO_2 has formed, most of the nitrogen atoms have been consumed to form NO by reaction with the much more abundant O_2*. Thus, N_2O chemiluminescence should likewise be small.

Recently, however, IR radiation from N_2O has been observed in the LABCEDE experiment (Reference 4-13) at AFGL in which air at moderately high pressures was bombarded by short pulses of electrons. The laboratory data could not be accounted for on the basis of the standard formation reaction above, but it has been suggested (Reference 4-13) that it may be explainable by the reaction

$$N_2(A^3\Sigma) + O_2 \longrightarrow N_2O + O \qquad (4\text{-}14)$$

where the $A^2\Sigma$ state of N_2 is formed in the experiment by the 3-body reaction

$$N + N + M \longrightarrow N_2(A^3\Sigma) + M \quad . \qquad (4\text{-}15)$$

If such is indeed the case, what are the implications for a nuclear environment? That is the question we now address.

First, since the radiative lifetime of $N_2(A)$ is only about 2 sec, the suggested mechanism can have significant duration only in regions where there exists a continuing production source for $N_2(A)$. This requirement restricts the possible applicability either to (low-altitude) highly dissociated fireballs, where Reaction 4-15 can operate, or to the γ- and β-patch regions in which excitation of $N_2(A)$ by electron impact is a continuing process.

---

* This statement should also apply to a multiburst environment.

Consider first the fireball region. For rapid formation of N_2O by the combination of Reactions 4-14 and 4-15, we need to have present, simultaneously, large concentrations of both atomic nitrogen and molecular oxygen. But, if the atomic nitrogen concentration is high (i.e. large fractional dissociation of the fireball), then the O_2 concentration will be small unless there is significant entrainment of the ambient air. If entrainment does effectively raise the O_2 concentration, then the nitrogen atoms are rapidly consumed by the O_2 to form NO and, consequently, in a short time will be unavailable to form $N_2(A)$ by Reaction 4-15. These statements are indeed borne out by detailed benchmark calculations performed with the FIRECHEM code. We conclude that the suggested mechanism is not significant in fireball regions except, perhaps, on a time scale too short for most practical applications.

Consider next the beta patch region in which $N_2(A)$ is produced continuously by electron bombardment of N_2. ARCTIC code calculations show that about 0.4 $N_2(A)$ molecules are produced by electron impact for each ion pair that is created. This number includes contributions from direct excitation of N_2 as well as from $C \rightarrow B \rightarrow A$ radiative cascade through the second- and first-positive band systems of nitrogen. We now apply this number to the case described previously (see discussion under NO^+) of a 1-MT fission-yield burst at 300-km altitude, 100 sec after the burst, with a debris radius of 500 km. As an upper limit, we assume steady state conditions in which each $N_2(A)$ molecule formed reacts with O_2 to produce, in the absence of quenching, one ν_3-band photon from N_2O. Thus, if q_e is the volume production rate of electrons by delayed β and γ rays, and Q is the quenching factor, the volume emission rate at 4.5 μm from N_2O is

$$\dot{\varepsilon}_{4.5\ \mu m} \sim 0.4\ q_e Q \quad (\text{photons cm}^{-3}\ \text{sec}^{-1}) \tag{4-16}$$

where

$$Q = \frac{A_{10}}{A_{10} + k_q[M]} \quad . \tag{4-17}$$

Here, A_{10} is the Einstein coefficient for the ν_3 band of N_2O, and $k_q[M]$ is the quenching rate. We assume that the quenching proceeds by V-V transfer to N_2 with a rate constant of 3×10^{-12} cm^2 sec^{-1} (as for NO^+). The value for A_{10} is 258 sec^{-1}. Using these numbers, and the previously computed values for q_e along a vertical path below the debris region, we obtain the following results.

For altitudes up to about 60 km, the zenith intensity is constant at about 2×10^{-10} watts cm^{-2} $ster^{-1}$ and then decreases with altitude to a value of about 5×10^{-12} at 100 km. These numbers are comparable to those quoted above for NO^+ emission because a comparable number of photons per ion pair was assumed for both species. Small though the numbers are, they are probably gross overestimates of the N_2O emission intensity since $N_2(A)$ will likely be quenched in other ways besides, perhaps, the formation of N_2O.

Uncertainties

The major uncertainties involved in chemiluminescent formation of N_2O by Reaction 4-14 are:

1. the rate constant for the Reaction 4-14
2. the effective number and spectral distribution of the emitted ν_3-band photons.
3. the quenching rates for the (00v) states of N_2O.

Recommendations

We do not recommend a measurement program for N_2O at this time. The foregoing considerations, incomplete though they may be, make it difficult for us to believe that IR emission near 4.5 μm from N_2O can ever be a serious threat to system performance. However, if it can be demonstrated that backgrounds, perhaps structured, of the magnitude quoted above are significant to a present or planned system, then a measurement program designed to reduce the above-listed uncertainties would certainly be in order.

SECTION 5
SUMMARY AND RECOMMENDATIONS

In order to improve the capability for predicting IR radiation at wavelengths from about 2 to 5 μm in a nuclear environment, we have attempted to isolate the dominant molecular emitters in that band, and to identify the factors that lead to the greatest uncertainty in the calculation of their radiant intensity. In so doing, we have restricted ourselves to uncertainties related solely to the chemical and optical properties of the disturbed air. Nevertheless, it is well to remember that uncertainties in the calculated emission, stemming from incomplete knowledge of the phenomenology of nuclear-burst-air interactions may, in some cases, dominate those considered here.*

Selection of the principal uncertainties is based on a study of the available evidence: field data (auroral and nuclear), recent laboratory measurements, results from code calculations, and discussions with co-workers. In the foregoing sections, a priority listing of the research needs was given for each molecule considered potentially significant in a nuclear environment. In this section, we attempt to provide an overall priority listing of the requirements, irrespective of molecule. Such a listing is necessarily influenced by an inherent bias with respect to the wavelength region deemed most important to systems. Our list is based partly on the assumption that the primary region is a band near 2.8 μm; the secondary region is a band near 4.3 μm. A different assumption would lead to a different ordering of the priorities.

---

* Even the presence of natural phenomena such as winds, turbulent diffusion, and vertical transport, that are difficult to predict and model, may drastically alter the spatial and temporal behavior of long-lived afterglow regions and lead to inherently large uncertainties. This is especially true in the case of CO_2 vibraluminescence.

For the band extending from about 2.6 to 2.9 μm we considered the species NO, CO_2, H_2O, OH, HO_2, H_2O_2, HNO_2, and HNO_3. Of these, NO has traditionally been considered the dominant emitter in a nuclear environment. However, in spite of all the experimental and theoretical efforts that have been directed toward a confirmation of this, doubt still persists because of inconsistencies between the NO mechanism and certain of the field data. The possibility that CO_2 vibraluminescence may be significant near 2.7 μm cannot yet be discounted. In this spectral region we give top priority to the need for positive species identification using interferometer techniques to achieve the required spectral resolution. Assuming that NO will prove to be the dominant emitter, we then rate the species (according to the need to acquire data relating to them) in the order: NO, CO_2, OH, H_2O, H_2O_2, HNO_3, HNO_2. No specific recommendations regarding the last four molecules in this list are given because it appears that their contribution (in the band considered here) to emission from a nuclear environment is small compared to that from the other species.

For the band extending from about 4.1 to 4.6 μm we considered the species CO_2, $N^{14}N^{15}$, NO^+, N_2O, and CO. Of these, the ν_3 band of CO_2 at 4.26 μm, excited mainly by vibrational transfer from N_2, is undoubtedly dominant, at least at altitudes below about 110 km. However, for potential systems operating at higher altitudes, or at wavelengths to the red side of 4.26 μm, emission from $N^{14}N^{15}$ and NO^+ may dominate, or at least compete with, emission from the hot bands and weak isotopic bands of CO_2. No specific recommendations are made for N_2O or CO. For N_2O, the only long-lasting source of excitation in a nuclear environment occurs in the beta patch for which we judge the N_2O chemiluminescence (including possible excitation by the $N_2(A) + O_2$ reaction) to be too small to be of practical concern. For CO, the main excitation mechanisms should be thermal collisions and/or earthshine scatter for which no great uncertainty exists with respect to the parameters involved.

Specific recommendations for research items, independent of the difficulty or feasibility of implementing them, are now listed in order of priority.

1. Perform field measurements of the spectral intensity in the 5.0 - 6.5-μm and 2.6 - 3.2-μm regions with sufficient resolution ($\lesssim 5\ cm^{-1}$) to unambiguously identify the radiating species in the disturbed atmosphere. The measurements should be made under conditions of intense auroral bombardment and/or in the afterglow region from an EXCEDE-type experiment.

2. Perform laboratory experiments to determine the branching ratios for production of $N(^4S)$ and $N(^2D)$ atoms (a) by dissociative recombination in N_2^+ and, (b) immediately following energy deposition by fast (keV) electrons.

3. Simultaneous with Item 1 above, make field measurements of the NO and O concentrations, especially in aurora.

4. Perform laboratory experiments to measure, simultaneously, the spectral intensity of CO_2 vibraluminescence near 2.7 and 4.3 μm. Vary the pressure over a sufficient range to establish the quenching factors involved.

5. Perform field measurements of the spectral intensity in the 4.1- to 4.8-μm region with sufficient resolution ($\lesssim 5\ cm^{-1}$) to unambiguously identify the radiating species. These measurements should be made as an integral part of the auroral or EXCEDE experiments recommended under Item 1 above. The experiment should determine the relative contributions from $N^{14}N^{15}$, NO^+, and the "hot" and isotopic bands of CO_2.

6. Perform laboratory experiments to determine the band strength for the fundamental of $N^{14}N^{15}$.

at 200-km altitude.

7. Perform laboratory experiments to determine rate constants, as functions of temperature, for the reactions

$$O + NO(v=0) \longrightarrow O + NO(v=1)$$
$$O + NO(v=0) \longrightarrow O + NO(v=2) \quad .$$

8. From laboratory measurements, determine rate constants for vibrational transfer from $N_2(v>1)$ to CO_2, and establish branching ratios for production of 4.3- and 2.7-μm radiation arising from the difference bands (hot bands) of CO_2.

9. Perform laboratory experiments to determine the vibrational distribution of NO^+ immediately following its formation by chemiluminescent reactions.

10. From laboratory measurements, determine the quenching rate of $N^{14}N^{15}(v)$ by V-V exchange with N_2 and by V-T collisions with atomic oxygen.

11. Measure the CO_2 mixing ratio at altitudes above 100 km.

12. Perform code calculations to confirm the tentative conclusion that in a nuclear environment the intensity of OH chemiluminescence is depressed below normal airglow levels.

13. Perform code calculations to confirm the tentative conclusion that HO_2 chemiluminescence is not important in a nuclear environment.

14. Perform laboratory experiments to determine the quenching rates for $NO(v>1)$ by O_2 and O.

15. Perform laboratory experiments, supplemental to those of Bien, to determine the quenching of $NO^+(v>3)$ by N_2 and also to establish, more conclusively, Einstein coefficients $A_{v,v-1}$ for NO^+.

REFERENCES

2-1. Archer, D. H., and P. W. Tarr, Auroral Simulation Studies, HAES Report No. 6, DNA 3567T, MRC-R-152, Mission Research Corporation, 22 April 1975.

2-2. Tarr, P. W., and D. H. Archer, Auroral Simulation Studies In Support of ICECAP and EXCEDE, HAES Report No. 24, DNA 3785F, MRC-R-211, Mission Research Corporation, 30 September 1975.

2-3. Archer, D. H., and P. W. Tarr, Final Report on Auroral Simulation Effects, HAES Report No. 62, DNA 4275F, MRC-R-313, Mission Research Corporation, 31 March 1977.

2-4. Kofsky, I. L., et al., Data Reduction and Auroral Characterizations for ICECAP III, HAES Report No. 59, DNA 4220F, Photometrics, Inc., 31 January 1977.

2-5. Kofsky, I. L., et al., Data Reduction and Auroral Characterizations for ICECAP II, HAES Report No. 27, DNA 3789F, Photometrics, Inc., 25 October 1975.

2-6. Huppi, R. J., and J. W. Reed, Aircraft Borne Measurements of Infrared Enhancements During ICECAP 1975 and 1976, HAES Report No. 68, AFGL-TR-77-0232, Utah State University, 28 September 1977.

2-7. Stair, A. T., HAES Infrared Data Review, AFGL-OP-TM-05, Vol. II, Meeting at Falmouth, Mass., 13-15 June 1977.

2-8. Myers, B. F., and M. R. Schoonover, Electron Energy Degradation In The Atmosphere, DNA 3513T, SAI-74-619-LJ, Science Applications, Inc., 3 January 1975.

2-9. Kley, D., et al., J. Geophys. Res. 66, 4157 (1977).

3-1. Oettinger, P. E., and K. P. Horn, J. Chem. Phys. 56, 1834 (1972).

3-2. Kumer, J. B., HAES Infrared Data Review Meeting, AFGL-OP-TM-05, Vol. II, Meeting at Falmouth, Mass., 13-15 June 1977.

3-3. James, T. C., Laboratory Investigation of Infrared Fluorescence of CO_2, HAES Report No. 69, DNA 4238F, Lockheed Palo Alto Research Laboratory, December 1976.

3-4. James, T. C., Lockheed Palo Alto Research Laboratory, Private Communication, April 1978.

3-5. Finzi, J., and C. B. Moore, J. Chem. Phys. 63, 2285 (1975).

3-6. Penner, S. S., Quantitative Molecular Spectroscopy and Gas Emissivities, Addison-Wesley (1959).

3-7. Grieder, W. F., et al., Rocket Measurement of OH Emission Profiles in the 1.56 and 1.99 μm Bands, HAES Report No. 38, AFCRL-TR-0057, Air Force Cambridge Research Laboratories, 28 January 1976.

3-8. Baker, D., HAES Infrared Data Review, AFGL-OP-TM-05, Vol. I, Meeting at Falmouth, Mass., 13-15 June 19755.

3-9. Moreels, G., et al., J. At. Terr. Phys. 39, 551 (1977).

3-10. Charters, R. E., et al., Appl. Optics 10, 1749 (1971).

3-11. Rogers, J. W., et al., J. Geophys. Res. 78, 7023 (1973).

3-12. Baker, Doran, Jr., and Allan J. Steed, J. Geophys. Res. 78, 8859 (1973).

4-1. James, T. C., and J. B. Kumer, J. Geophys. Res. 78, 8320 (1973).

4-2. Kumer, J. B., Further Evaluation of ICECAP Auroral 4.3 μm Zenith Radiance, HAES Report No. 57, DNA 4260F, Lockheed Palo Alto Research Laboratory, October 1976.

4-3. Kumer, J. B., J. Geophys. Res. 82, 2203 (1977).

4-4. Garstang, R. H., Atomic and Molecular Processes (Edited by D. R. Bates), Chap. 1, Academic Press, New York (1962).

4-5. Bates, D. R., and G. Poots, Proc. Phys. Soc. A66, 784 (1953).

4-6. Wu, T-Y, Can. J. Phys. 30, 291 (1952).

4-7. Gordiets, et al., Preprint No. 84-1976, Physics of High Energy and Cosmic Radiation, Lebedev Physical Institute of the USSR Academy of Sciences, Moscow.

4-8. Kennealy, J., HAES Infrared Data Review, AFGL-OP-TM-05, Vol. I, Meeting at Falmouth, Mass., 13-15 June 1977.

4-9. DNA Reaction Rate Handbook, DNA 1948H, Revision No. 6, December 1975.

4-10. Knapp, W. S., and P. G. Fischer, Aids For The Study of Electromagnetic Blackout, DASA 2499, July 1970.

4-11. Bien, Fritz, Measurements of Nitric Oxide Ion Vibrational Absorption Coefficient and Vibrational Transfer to N_2, AFGL-TR-77-0181, Aerodyne Research, Inc., September 1977.

4-12. Billingsley, Frank P. II, Chem. Phys. Lett. 23, 160 (1973).

4-13. Caledonia, G. E., HAES Infrared Data Review, AFGL-OP-TM-05, Vol. I, Meeting at Falmouth Mass., 13-15 June 1977.

APPENDIX A
PHOTONS PER $N(^2D) + O_2$ REACTION

A determination of the average number of photons produced per $N(^2D) + O_2 \rightarrow NO + O$ reaction in the fundamental and overtone bands of NO, using the recent COCHISE data (Reference 4-8), proceeds as follows.

ZERO QUENCHING LIMIT

Let n be the highest vibrational state populated by the reaction. From energy conservation, $n = 18$. However, the maximum level seen in the COCHISE experiments is $n = 12$, a value that we will adopt here. If we ignore collisional excitation and de-excitation, the steady state population of state v, $[N_2(v)]$, is determined by a balance between production from a combination of the chemiluminescent reaction and radiative cascade from higher levels, and by destruction from radiative decay to lower levels. Thus,

$$[N_2(n)] = \frac{P(n)}{A_{n,n-1} + A_{n,n-2}} \tag{A-1}$$

where $P(n)$ is the production rate of state n by the chemical reaction, and $A_{n,n-1}$ and $A_{n,n-2}$ are the Einstein rates of spontaneous emission. Similarly,

$$[N_2(n-1)] = \frac{P(n-1) + A_{n,n-1}[N_2(n)]}{A_{n-1,n-2} + A_{n-1,n-3}} \tag{A-2}$$

$$[N_2(v)] = \frac{P(v) + A_{v+1,v}[N_2(v+1)] + A_{v+2,v}[N_2(v+2)]}{A_{v,v-1} + A_{v,v-2}} \quad ; \; v = 2, 3, \ldots, n-2 \tag{A-3}$$

$$\vdots$$

$$[N_2(1)] = \frac{P(1) + A_{2,1}[N_2(2)] + A_{3,1}[N_2(3)]}{A_{1,0}} \; . \tag{A-4}$$

Let k_v be the rate constant for the reaction

$$N(^2D) + O_2 \xrightarrow{k_v} NO(v) + O \quad . \tag{A-5}$$

If k is the overall rate constant, then

$$k_v = f_v k \tag{A-6}$$

where the fraction, f_v, which is the probability per reaction of populating state v, must satisfy the relation

$$\sum_{v=0}^{n} f_v = 1 \quad . \tag{A-7}$$

Define now the quantity $G(v)$ such that

$$G(v) = \frac{[N_2(v)]}{k[N(^2D)][O_2]} \quad . \tag{A-8}$$

Then, from Equations A-3 and A-8, we can write

$$G(v) = \frac{f_v + A_{v+1,v}G(v+1) + A_{v+2,v}G(v+2)}{A_{v,v-1} + A_{v,v-2}} \quad ; \quad v = 2,3,\ldots,n-2 \quad . \tag{A-9}$$

Corresponding relations for $G(n)$, $G(n-1)$, and $G(1)$ follow from Equations A-1, A-2, and A-4.

Since the steady state volume emission rates for the fundamental and overtone bands are given, respectively, by

$$\dot{\phi}_{fund.} = \sum_{v=1}^{n} A_{v,v-1}[N_2(v)] \tag{A-10}$$

and

$$\dot{\phi}_{overtone} = \sum_{v=2}^{n} A_{v,v-2}[N_2(v)] \quad , \tag{A-11}$$

it follows that the number of photons per reaction, η, emitted in the fundamental and overtone bands are given, respectively, by

$$\eta_{\text{fund.}} = \sum_{v=1}^{n} \eta_{v,v-1} = \sum_{v=1}^{n} A_{v,v-1} G(v) \qquad \text{(A-12)}$$

$$\eta_{\text{overtone}} = \sum_{v=2}^{n} \eta_{v,v-2} = \sum_{v=2}^{n} A_{v,v-2} G(v) \quad . \qquad \text{(A-13)}$$

In Table A-1 are listed the ingredients that go into a determination of $\eta_{\text{fund.}}$ and η_{overtone}. $P'(v)$ is the relative production rate of state v as determined by the COCHISE experiments (Reference 4-8). The value of $P'(0)$ was not measured but, by extrapolation, is assumed equal to that for states $v = 2$ through 5. The data shown in Reference 4-8 gives a value for $P'(v)$ of about 1.4, but later work by AFGL (Reference A-1) indicates that it should be closer to 1.0 as it is for states $v = 2$ through 5. This gives support for the assumption that $P'(0)$ is also close to unity. The values for the Einstein coefficients are taken from a paper by Billingsley (Reference A-2).

As seen from Table A-1, the results (to two significant figures), in the zero quenching limit, are:

$$\eta_{\text{fund.}} = 3.9 \text{ (photons/reaction)}$$

$$\eta_{\text{overtone}} = 0.28 \text{ (photons/reaction)}$$

CASE WITH QUENCHING

The foregoing results can readily be modified to include quenching provided a suitable quenching model is adopted. According to the literature,

Table A-1. Ingredients for determination of η from Equations A-12 and A-13.

v	P'(v)	f_v	$A_{v,v-1}$ (sec^{-1})	$A_{v,v-2}$ (sec^{-1})	G(v) (sec)	$\eta_{v,v-1}$	$\eta_{v,v-2}$
0	1.0 (assumed)	.1044					
1	1.0	.1044	10.78		$8.085^{-2(*)}$	8.716^{-1}	
2	1.0	.1044	20.43	0.46	3.635^{-2}	7.427^{-1}	1.672^{-2}
3	1.0	.1044	29.11	1.51	2.105^{-2}	6.129^{-1}	3.179^{-2}
4	1.0	.1044	36.49	3.10	1.359^{-2}	4.958^{-1}	4.212^{-2}
5	1.0	.1044	42.93	4.90	9.077^{-3}	3.897^{-1}	4.447^{-2}
6	0.94	.0982	48.54	7.29	6.018^{-3}	2.921^{-1}	4.387^{-2}
7	0.94	.0982	53.54	9.63	3.908^{-3}	2.092^{-1}	3.763^{-2}
8	0.78	.0815	57.48	12.50	2.284^{-3}	1.313^{-1}	2.854^{-2}
9	0.40	.0418	60.55	15.68	1.110^{-3}	6.720^{-2}	1.740^{-2}
10	0.25	.0261	62.77	19.14	5.801^{-4}	3.641^{-2}	1.110^{-2}
11	0.15	.0158	64.15	22.94	2.784^{-4}	1.786^{-2}	6.387^{-3}
12	0.114	.0120	64.61	27.15	1.308^{-4}	8.450^{-3}	3.551^{-3}
						$\sum_v = 3.88$	$\sum_v = 0.284$

*Superscripts denote powers of ten.

the main atmospheric quenchers of NO(v) are atomic and molecular oxygen. We therefore assume the quenching reactions are

$$NO(v) + O_2 \xrightarrow{k^{(1)}_{v,v-1}} NO(v-1) + O_2 \qquad \text{(A-14)}$$

$$NO(v) + O \xrightarrow{k^{(2)}_{v,v-1}} NO(v-1) + O \quad . \qquad \text{(A-15)}$$

These reactions serve to de-excite level v and populate level v-1. Whether Reaction A-14 is of the V-T or V-V type is not too significant for our purposes.

The functions G(v), defined by Equation A-9, are now modified as follows:

$$G(n) = \frac{f_n}{A_{n,n-1} + A_{n,n-2} + k^{(1)}_{n,n-1}[O_2] + k^{(2)}_{n,n-1}[O]} \qquad \text{(A-16)}$$

$$G(n-1) = \frac{f_{n-1} + (A_{n,n-1} + k^{(1)}_{n,n-1}[O_2] + k^{(2)}_{n,n-1}[O])G(n)}{A_{n-1,n-2} + A_{n-1,n-3} + k^{(1)}_{n-1,n-2}[O_2] + k^{(2)}_{n-1,n-2}[O]} \qquad \text{(A-17)}$$

$$\vdots$$

$$G(v) = \frac{f_v + (A_{v+1,v} + k^{(1)}_{v+1,v}[O_2] + k^{(2)}_{v+1,v}[O])G(v+1) + A_{v+2,v}G(v+2)}{A_{v,v-1} + A_{v,v-2} + k^{(1)}_{v,v-1}[O_2] + k^{(2)}_{v,v-1}[O]} \; ; v=2,3,\ldots,n-2 \qquad \text{(A-18)}$$

$$\vdots$$

$$G(1) = \frac{f_1 + (A_{2,1} + k^{(1)}_{2,1}[O_2] + k^{(2)}_{2,1}[O])G(2) + A_{3,1}G(3)}{A_{1,0} + k^{(1)}_{1,0}[O_2] + k^{(2)}_{1,0}[O]} \qquad \text{(A-19)}$$

These expressions can now be used in Equations A-12 and A-13 to determine the photon yield once values for the quenching rate constants are specified.

In order to test the sensitivity of the results to changes in the quenching, we adopt here two different models: one where the quenching rate constant is proportional to the vibrational state v; the other where it is independent of v.

Model I : $k_{v,v-1} = vk_{1,0}$

Here we assume the following rate constants ($cm^3 sec^{-1}$):

$$k_{1,0}^{(1)} = 2.4 \times 10^{-14} \quad \text{(Reference A-3)}$$

$$k_{1,0}^{(2)} = 4 \times 10^{-11} \quad \text{(inferred from Reference A-4; also see Reference A-5).}$$

Model 2 : $k_{v,v-1} = k_{1,0}$

In this case we take

$$k_{1,0}^{(1)} = 4.2 \times 10^{-14} \quad \text{(Reference A-3)}$$

$$k_{1,0}^{(2)} = 4 \times 10^{-11} \quad .$$

These two quenching models have been utilized in the foregoing equations to compute values for η, and for $\eta_{v,v-1}$, and $\eta_{v,v-2}$, at selected altitudes between 20 and 160 km. The results are shown in Figures A-1 to A-3.

Figure A-1 gives the total number of photons emitted per reaction in the fundamental and first overtone bands. At high altitudes the curves properly approach the zero quenching limits. Below 80 km, the photon yield rapidly decreases because of O_2 quenching. The minimum that occurs at 100 km is due to quenching by atomic oxygen whose concentration was assumed to peak at that altitude. Quenching by this species evidently accounts for the major difference near 100 km between our

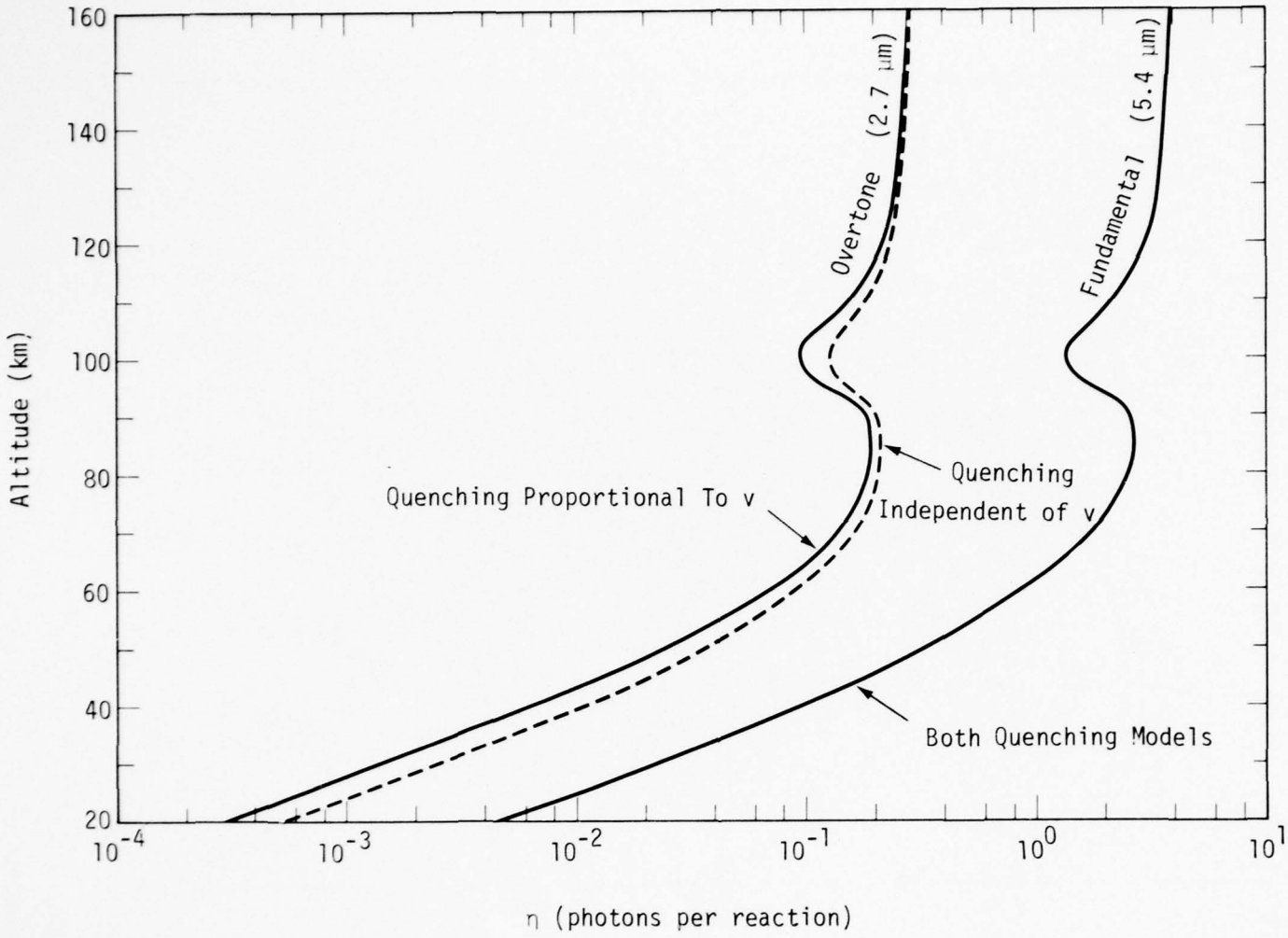

Figure A-1. Calculated number of photons emitted from NO per $N(^2D) + O_2 \rightarrow NO + O$ reaction for two different quenching models.

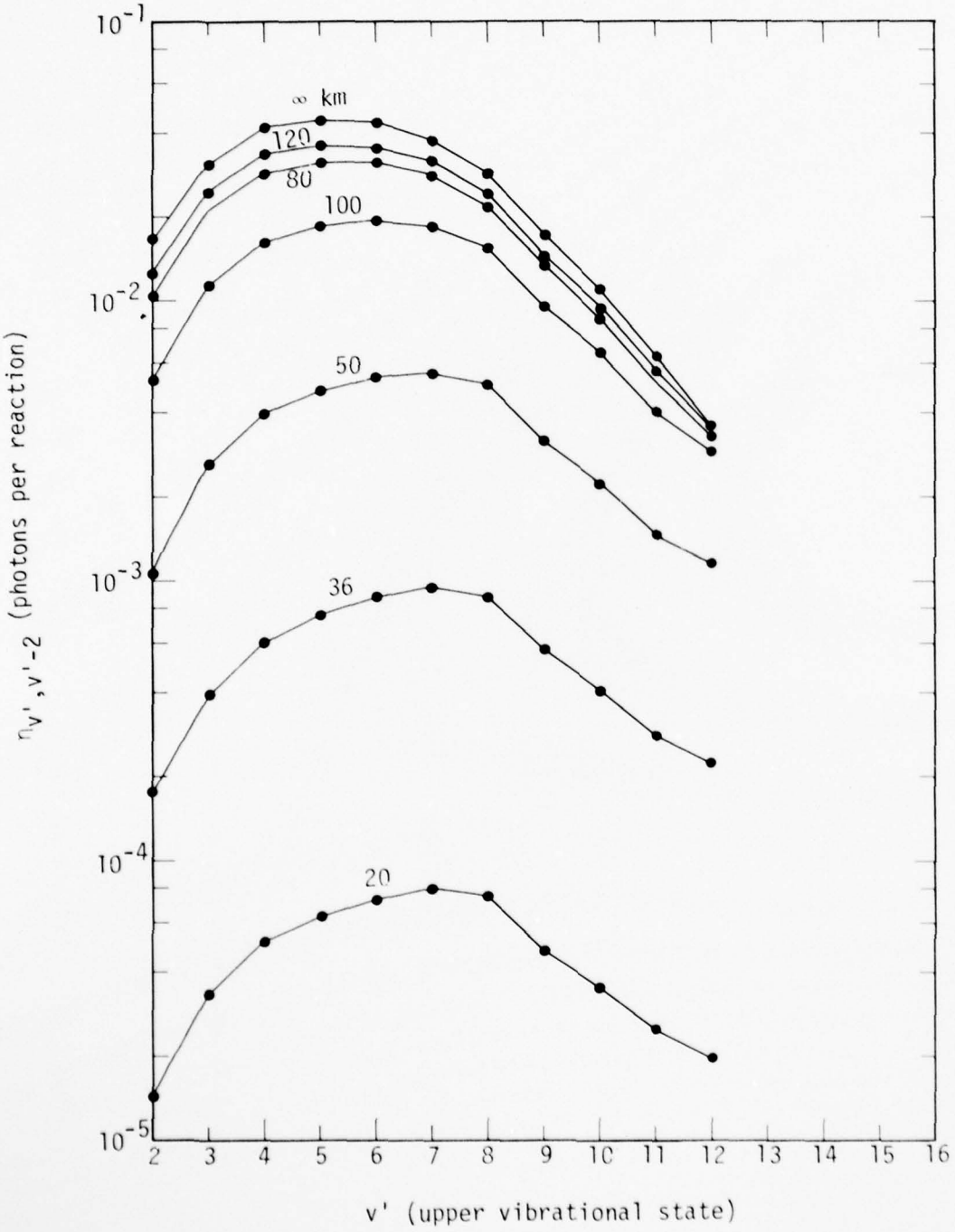

Figure A-2. NO overtone photons per $N(^2D) + O_2 \rightarrow NO + O$ reaction at selected altitudes (quenching model independent of v).

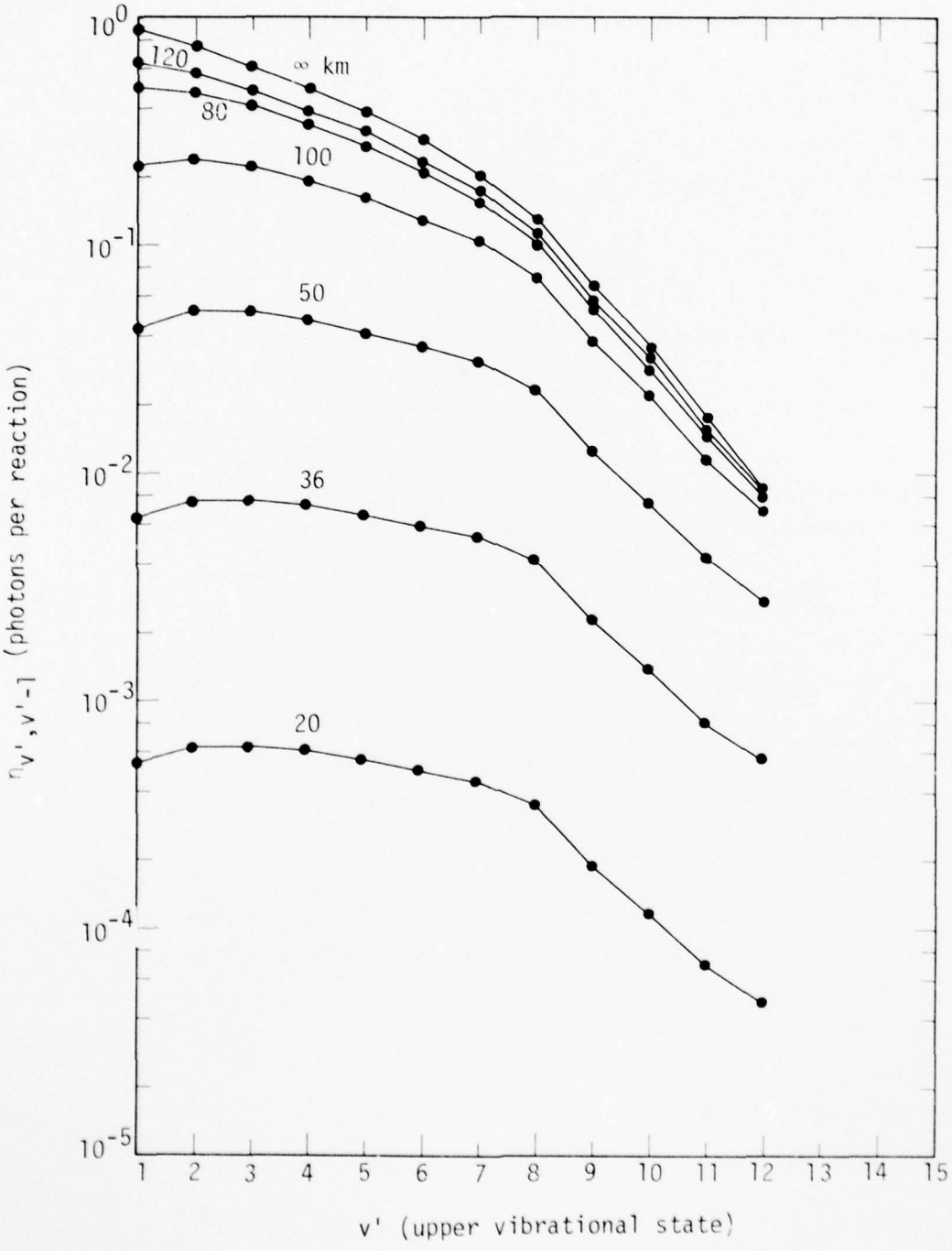

Figure A-3. NO fundamental photons per $N(^2D) + O_2 \rightarrow NO + O$ reaction at selected altitudes (quenching model independent of v).

results and those presented in Reference 4-8 by Kennealy, which amounts to nearly a factor of three. At 80 km, however, where O_2 is the dominant quencher, the two results are quite similar.

For the fundamental band, the two quenching models give results that differ by at most 5 or 6 percent. In Figure A-1, in fact, they are merged into a single curve. For the overtone band, the results for the two models are at least distinguishable. At 20-km altitude the difference is about 70 percent, but it decreases with increasing altitude. The main point to note here is that unless the quenching rate varies with the vibrational quantum number, v, much faster than v, the results are fairly insensitive to the details of the variation.

Figures A-2 and A-3 show the photon yields for individual transitions of the overtone and fundamental band systems, respectively, calculated using Model 2 quenching. Apart from the seemingly out-of-sequence position of the curve for 100-km altitude (due to O-atom quenching) in each of the figures, the main point to note, especially in Figure A-2, is the shift of the peak emission to higher vibrational states with decreasing altitude. For the overtone band at high altitudes, the peak emission is produced by the (5,3) band (2.81 μm). At and below 50 km, however, it is produced by the (7,5) band (2.90 μm). Thus, with Model 2 quenching, one would expect a shift in the chemiluminescent overtone spectrum to longer wavelengths as the altitude is decreased. However, for Model 1 quenching, our detailed results (not shown) show that the peak overtone emission is produced by the (5,3) band of NO at all altitudes. In this case we would expect little or no shift in the spectrum with changes in altitude.

REFERENCES

A-1. Del Greco, Frank P., AFGL, Private Communication, March 1978.

A-2. Billingsley, Frank P. II, J. Mol. Spectr. 61, 53 (1976).

A-3. Murphy, R. E., et al., J. Chem. Phys. 63, 2919 (1975).

A-4. Degges, T., HAES Infrared Data Review, AFGL-OP-TM-05, Vol. I, Meeting at Falmouth, Mass., 13-15 June 1977.

A-5. Glänzer, K., and J. Troe, J. Chem. Phys. 63, 4352 (1975).

DISTRIBUTION LIST

DEPARTMENT OF DEFENSE

Assistant to the Secretary of Defense
Atomic Energy
ATTN: Executive Assistant

Defense Advanced Rsch. Proj. Agency
ATTN: S. Zakanyc
ATTN: W. Whitaker
ATTN: STO
ATTN: G. Canavan

Defense Documentation Center
Cameron Station
12 cy ATTN: TC

Defense Nuclear Agency
ATTN: RAAE, J. Mayo
ATTN: RAEV, H. Fitz, Jr.
ATTN: RAAE, R. Bigoni
ATTN: DDST
3 cy ATTN: RAAE, C. Blank
4 cy ATTN: TITL

Field Command
Defense Nuclear Agency
ATTN: FCPR

Livermore Division, Field Command, DNA
Department of Defense
Lawrence Livermore Laboratory
ATTN: FCPRL

Under Secretary of Defense for Rsch. & Engrg.
Department of Defense
ATTN: Strategic & Space Systems (OS)

DEPARTMENT OF THE ARMY

Atmospheric Sciences Laboratory
U.S. Army Research & Development Command
3 cy ATTN: H. Ballard
3 cy ATTN: DELAS-EO, F. Niles

BMD Advanced Technology Center
Huntsville Office
Department of the Army
ATTN: ATC-O, W. Davies
ATTN: ATC-T, M. Capps

Deputy Chief of Staff for Rsch. Dev. & Acq.
Department of the Army
ATTN: Nuclear Team
ATTN: DAMA-WSZ-C
ATTN: DAMA-CSZ-C

FRADCOM Technical Support Activity
Department of the Army
ATTN: S. Kronenberg
ATTN: Inst. for Exploratory Res.
ATTN: Wpns. Effects Section
5 cy ATTN: DRSEL

Harry Diamond Laboratories
Department of the Army
2 cy ATTN: DELHD-NP, F. Wimenitz

DEPARTMENT OF THE ARMY (Continued)

U.S. Army Ballistic Research Labs
ATTN: J. Mester
ATTN: Technical Library

U.S. Army Foreign Science & Tech. Ctr.
ATTN: B. Smith

U.S. Army Nuclear & Chemical Agency
ATTN: Library

U.S. Army Research Office
2 cy ATTN: CRDARD-P, R. Mace

DEPARTMENT OF THE NAVY

Naval Electronic Systems Command
ATTN: PME 117

Naval Intelligence Support Ctr.
ATTN: Document Control

Naval Ocean Systems Center
ATTN: Code 2200, H. Hughes
ATTN: Code 2200, R. Pappert
ATTN: Code 2200, J. Richter
ATTN: Code 2200, I. Rothmuller
ATTN: Code 2200, W. Moler

Naval Postgraduate School
ATTN: Code 2124, Tech. Rpts. Librarian

Naval Research Laboratory
ATTN: Code 6750, J. Davis
ATTN: Code 2627
ATTN: Code 7750, J. Fedder
ATTN: Code 7127, C. Johnson
ATTN: Code 7700, T. Coffey
ATTN: Code 7126, D. McNutt
ATTN: Code 7709, W. Ali
ATTN: Code 7701, J. Brown
ATTN: Code 6750, D. Strobel
ATTN: Code 7750, S. Ossakow

Naval Surface Weapons Center
ATTN: Code F31

DEPARTMENT OF THE AIR FORCE

Aeronautical Systems Division, AFSC
ATTN: ASD-YH-EX, R. Leverette

Air Force Geophysics Laboratory
ATTN: OPR, A. Stair
ATTN: PHG, J. McClay
2 cy ATTN: LKO, R. Huffman
2 cy ATTN: OPR, J. Kennealy
2 cy ATTN: OPR, R. Murphy
3 cy ATTN: LKD, R. Narcisi
5 cy ATTN: OPR-1, J. Ulwick
10 cy ATTN: LKB, K. Champion

Air Force Technical Applications Center
2 cy ATTN: STINFO Office/TF

AD-A061 430 MISSION RESEARCH CORP SANTA BARBARA CALIF F/G 18/3
REQUIREMENTS FOR IMPROVED INFRARED PREDICTION CAPABILITY. HAES --ETC(U)
APR 78 D H ARCHER DNA001-77-C-0227
UNCLASSIFIED MRC-R-383 DNA-4585F NL

2 OF 2
AD
A061 430

END
DATE
FILMED
2-79
DDC

DEPARTMENT OF THE AIR FORCE (Continued)

Air Force Systems Command
ATTN: DLTW
ATTN: DLCAW
ATTN: DLS
ATTN: Technical Library
ATTN: SDR
ATTN: DLXP

Air Force Weapons Laboratory
ATTN: SUL
ATTN: DYT, D. Mitchell
2 cy ATTN: DES, G. Ganong

Deputy Chief of Staff
Research, Development, & Acq.
Department of the Air Force
3 cy ATTN: AFRDQ

Rome Air Development Center
Air Force Systems Command
3 cy ATTN: OCSE, J. Simons

Space & Missile Systems Organization/AW
Air Force Systems Command
16 cy ATTN: AWW

Space & Missile Systems Organization/SZ
Air Force Systems Command
ATTN: SZJ

DEPARTMENT OF ENERGY

Argonne National Laboratory
Records Control
ATTN: Doc. Con. for Lib. Svcs. Rpts. Sec.

Department of Energy
Library Room G-042
ATTN: Doc. Con. for Classified library

Lawrence Livermore Laboratory
ATTN: Doc. Con. for L-142, D. Wuebbles
ATTN: Doc. Con. for L-404, W. Duewer
ATTN: Doc. Con. for L-404, G. Haugan
ATTN: Doc. Con. for L-71, J. Chang

Los Alamos Scientific Laboratory
ATTN: Doc. Con. for W. Maier
ATTN: Doc. Con. for Reference Lib., A. Beyer
ATTN: Doc. Con. for R. Brownlee
ATTN: Doc. Con. for R. Jeffries
ATTN: Doc. Con. for M. Tierney
ATTN: Doc. Con. for C. Mehl
ATTN: Doc. Con. for H. Argo

Office of Military Application
Department of Energy
ATTN: Document Control

Sandia Laboratories
Livermore Laboratory
ATTN: Doc. Con. for T. Cook

Sandia Laboratories
ATTN: Doc. Con. for L. Anderson
ATTN: Doc. Con. for 3141
ATTN: Doc. Con. for M. Kramm
ATTN: Doc. Con. for W. Brown

OTHER GOVERNMENT AGENCIES

Albany Metallurgy Research Center
U.S. Bureau of Mines
ATTN: E. Abshire

Central Intelligence Agency
ATTN: RD/SI, Rm. 5G48, Hq. Bldg. for
NED/OSI-2G48 Hqs.

Department of Commerce
National Bureau of Standards
ATTN: S. Abramowitz
ATTN: J. Devoe
ATTN: M. Krauss
ATTN: L. Gevantman
ATTN: G. Sinnatt
ATTN: J. Cooper
ATTN: K. Kessler

Department of Transportation
Office of the Secretary
ATTN: S. Coroniti

Institute for Telecommunications Sciences
National Telecommunications & Info. Admin.
ATTN: W. Utlaut

National Aeronautics and Space Administration
Goddard Space Flight Center
ATTN: A. Tempkin
ATTN: J. Siry
ATTN: S. Bauer
ATTN: Technical Library
ATTN: J. Heppner
3 cy ATTN: A. Aiken

National Aeronautics and Space Administration
George C. Marshall Space Flight Center
ATTN: R. Chappell
ATTN: J. Watts
ATTN: C. Balcher
ATTN: R. Hudson
ATTN: W. Oran
ATTN: N. Stone
ATTN: W. Roberts

National Aeronautics and Space Administration
ATTN: R. Fellows
ATTN: D. Hallenbeck
ATTN: D. Cauffman
ATTN: A. Schardt
ATTN: M. Tepper
ATTN: A. Gessow

National Aeronautics and Space Administration
Langley Research Center
ATTN: C. Schexnayder

National Aeronautics and Space Administration
Ames Research Center
ATTN: W. Starr
ATTN: R. Whitten
ATTN: N. Farlow
ATTN: G. Poppoff

National Aeronautics and Space Administration
Wallops Flight Center
ATTN: J. Gray

OTHER GOVERNMENT AGENCIES (Continued)

National Oceanic & Atmospheric Admin.
Environmental Research Laboratories
Department of Commerce
3 cy ATTN: E. Fehsenfeld
3 cy ATTN: E. Ferguson

DEPARTMENT OF DEFENSE CONTRACTORS

Aero-Chem Research Labs, Inc.
ATTN: A. Fontijn
ATTN: H. Pergament

Aerodyne Research, Inc.
Bedford Research Park
ATTN: F. Bien
ATTN: M. Camac

Aerospace Corporation
ATTN: T. Widhoph
ATTN: T. Taylor
ATTN: H. Mayer
ATTN: V. Josephson
ATTN: S. Kash
ATTN: N. Cohen
ATTN: R. McNeal
ATTN: R. Grove
ATTN: I. Garfunkel
ATTN: F. Morse
ATTN: J. Reinheimer

Avco Everett Research Laboratory, Inc.
ATTN: G. Sutton
ATTN: C. Von Rosenberg, Jr.
ATTN: A830

Battelle Memorial Institute
ATTN: R. Thatcher
ATTN: D. Hamman
ATTN: STOIAC

Berkeley Research Associates, Inc.
ATTN: J. Workman

Boston College
2 cy ATTN: Chairman, Dept. of Chem.
2 cy ATTN: Chairman, Dept. of Physics

Brown Engineering Company, Inc.
Cummings Research Park
ATTN: N. Passino

University of California at Riverside
ATTN: A. Lloyd
ATTN: J. Pitts, Jr.

California Institute of Technology
Jet Propulsion Lab
ATTN: J. Ajello

State of California
Air Resources Board
ATTN: L. Zafonte

University of California
Berkeley Campus
ATTN: H. Johnston
ATTN: Dept. of Chem., W. Miller
ATTN: F. Mozer

DEPARTMENT OF DEFENSE CONTRACTORS (Continued)

Calspan Corporation
ATTN: M. Dunn
ATTN: C. Treanor
ATTN: G. Valley
ATTN: W. Wurster

University of Colorado
Office of Contracts and Grants
ATTN: J. Pearce
ATTN: C. Barth
ATTN: A. Phelps
ATTN: C. Beaty
ATTN: C. Lineberger

Columbia University
ATTN: Sec. Officer, H. Foley

Columbia University
La Mont Doherty Geological Observatory
ATTN: B. Phelan

Concord Sciences
ATTN: E. Sutton

Cornell University
Department of Electrical Engineering
ATTN: M. Kelly

University of Denver
Colorado Seminary
Denver Research Institute
ATTN: Sec. Officer for V. Zyl
ATTN: Sec. Officer for D. Murcray

Environmental Rsch. Inst. of Michigan
ATTN: IRIA, Library

General Electric Company
Space Division
Valley Force Space Center
ATTN: F. Alyea
ATTN: T. Baurer
ATTN: Space Sci. Lab., M. Bortner
ATTN: P. Zavitsanos
ATTN: J. Burns
ATTN: R. Edsall

General Electric Company-TEMPO
Center for Advanced Studies
ATTN: T. Stephans
ATTN: D. Chandler
ATTN: W. Knapp
ATTN: B. Gambill
ATTN: J. Jordano
5 cy ATTN: DASIAC

General Research Corporation
Santa Barbara Division
ATTN: J. Ise, Jr.

Geophysical Institute
University of Alaska
ATTN: Physics Dept., J. Wagner
ATTN: B. Watkins
ATTN: R. Parthasarathy
ATTN: T. Davis
ATTN: D. Henderson
3 cy ATTN: N. Brown

DEPARTMENT OF DEFENSE CONTRACTORS (Continued)

Institute for Defense Analyses
ATTN: H. Wolfhard
ATTN: E. Bauer

Lockheed Missiles and Space Company, Inc.
ATTN: R. Johnson
ATTN: J. Kumer
ATTN: J. Cladis
ATTN: T. James
ATTN: J. Reagan
ATTN: B. McCormac
ATTN: M. Walt
ATTN: R. Sears

University of Lowell
Center for Atmospheric Research
ATTN: G. Best

University of Minnesota
ATTN: J. Winkler

Mission Research Corporation
ATTN: M. Scheibe
ATTN: D. Sappenfield
ATTN: R. Fischer
5 cy ATTN: D. Sowle
5 cy ATTN: Document Control
10 cy ATTN: D. Archer

Photometrics, Inc.
ATTN: I. Kofsky

Physical Dynamics, Inc.
ATTN: A. Thompson

Physical Science Laboratory
ATTN: W. Berning

Physical Sciences, Inc.
ATTN: G. Caledonia
ATTN: R. Taylor
ATTN: K. Wray

Physics International Company
ATTN: Doc. Con. for Technical Library

University of Pittsburgh
Cathedral of Learning
ATTN: F. Kaufman
ATTN: E. Gerjudy
ATTN: W. Fite
ATTN: M. Biondi

The Trustees of Princeton University
Forrestal Campus Library
ATTN: A. Kelly

R&D Associates
ATTN: H. Mitchell
ATTN: J. Rosengren

The Rand Corporation
ATTN: C. Crain

DEPARTMENT OF DEFENSE CONTRACTORS (Continued)

R&D Associates
ATTN: C. MacDonald
ATTN: R. Latter
ATTN: R. Lindgren
ATTN: R. Turco
ATTN: R. Lelevier
ATTN: H. Ory
ATTN: A. Latter
ATTN: D. Dee
ATTN: B. Gabbard
ATTN: F. Gilmore

Science Applications, Inc.
ATTN: D. Hamlin
ATTN: D. Sachs

Space Data Corporation
ATTN: E. Allen

SRI International
ATTN: W. Chesnut
ATTN: R. Leadabrand
ATTN: M. Baron
ATTN: D. McDaniels

SRI International
ATTN: C. Hulbert

Technology International Corporation
ATTN: W. Boquist

United Technologies Corporation
ATTN: R. Bullis
ATTN: H. Michels

Utah State University
Contract/Grant Office
ATTN: Sec. Officer for D. Burt
ATTN: Sec. Officer for C. Wyatt
3 cy ATTN: Sec. Officer for K. Baker
3 cy ATTN: Sec. Officer for D. Baker

VisiDyne, Inc.
ATTN: J. Carpenter
ATTN: H. Smith
ATTN: T. Degges
ATTN: W. Reidy
ATTN: C. Humphrey

Wayne State University
ATTN: R. Kummler

Wayne State University
Department of Physics
ATTN: W. Kauppila

Yale University
ATTN: Engineering Department